F.L.C.S.

Fabric **L**aser **C**utting **S**ystem

Department of Electrical and Computer Engineering
Department of Optics and Photonics

EEL 4914 – Senior Design I
Fall 2025 – Spring 2026

Group 2 Team:

Jacqueline Harper	Nolphky Nicolas	Michael Rodriguez	Anthony Martinez-Garcia
Photonic Science and Engineering	*Computer Engineering*	*Photonic Science and Engineering*	*Electrical Engineering*

Review Committee:

Dr. Peter Delfyett	CREOL	Pegasus Professor
Prof. Maddox	ECE	Instructor
Dr. Hao Zheng	ECE	Assistant Professor
Dr. Suboh Suboh	ECE	Associate Lecturer

Advisors:

Dr. Saleem Sahawneh	ECE	Lecturer
Dr. Aravinda Kar	CREOL	Professor

List of Figures

List of Tables

Chapter 2: Project Description

2.1 Motivation & Background

The idea of F.L.C.S. is a solution solver. The design of this fabric laser cutter will appeal to those who do not have advanced understanding of computers or computer softwares. Instead of needing a cutting software or specific file or a laptop to upload the desired cut pattern, we can instead use image acquisition and processing to differentiate the desired cut lines from the fabric. This product is for those "old-fashioned" hobbyists who might want some technology to assist them in physically cutting, without needing the background knowledge needed for operating software and uploading files.

F.L.C.S can be useful for all types of hobbyists, designers, and manufacturers who desire quick cutting of pieces of fabric at the tap of a screen. By drawing using a black marker on light fabric or white on dark fabric, the user can outline the desired shape of their fabric and click the touchscreen module to cut the desired lines once the fabric is inside the machine. It is large enough to have a variety of practical applications in terms of the large area we are able to cut. If needed, the system can run multiple cuts on the object.

In senior design our objective is to gather and work as a group. With this project multiple subsystems will be utilized, including a laser diode system, mirror guidance system, power systems, and a user-friendly touchscreen. The beam from the laser diode is focused and collimated using the lens system and is directed by the mirror system. The housing includes a user-friendly touchscreen as well as an optical system emergency stop switch. F.L.C.S's design allows for expansion of its' subsystems if needed, to accommodate the students in the group. For users, this system will be easy to use and understand. It will fit on your work desk or fabric station and will not require you to connect your laptop or PC for fabric cutting.

2.2 Existing Projects & Prior Related Work

2.2.1 Open Source Buildlog.net 2.x Laser [1]

The Buildlog 2.x laser is a second generation open-source laser cutter that employs a 2-axis rail-based XY gantry system, with an additional manually adjustable vertical axis. Unlike our proposed fabric laser cutter, the Buildlog 2.x does not have a Human-Machine Interface (HMI). Instead, it relies on tethered computer control for job setup and execution. Our design introduces an onboard Raspberry Pi touchscreen HMI to enable stand-alone operation, real-time job management, and user feedback without requiring a connected computer. In addition, while the Buildlog design delivers the laser via a moving gantry, our project employs mirrors that will steer the beam to the appropriate destination. This approach should reduce the mechanical load of moving the entire laser head and potentially enabling faster operation, though it introduces new challenges in precision alignment and control. Despite these differences, the Buildlog 2.x website provides valuable reference material for general mechanical layout, enclosure design, and community-tested best practices that we can include in our own system.

2.2.2 Commercial Epilog Fusion Pro Lasers [2]

The Epilog Fusion Pro is a professional, industry-level laser cutter that integrates a built-in touchscreen HMI, similar to what we intend to implement in our project. Its 7" display allows a user to select between stored jobs, adjust parameters, auto-focus the laser, and rerun previous cuts directly from the machine without requiring a tethered computer**.** In addition, the Fusion Pro incorporates an overhead camera system, which provides a real-time view of the work area. These features align with our project goals for the CLOTH system. By adding an onboard touchscreen interface, our cutter will provide stand-alone job management and ease of use comparable to the Fusion Pro. Although we will not reach the same industrial-grade specifications; we seek to emulate their machine on a smaller and cheaper scale.

2.2.3 DENER FiBER LASER [3]

The DENER FiBER LASER is a high-performance 2D metal sheet cutter designed for industrial applications. It uses an XYZ moving gantry laser system, allowing for precise and efficient cutting across large sheet areas. The machine integrates with custom CAD/CAM software, enabling operators to import digital designs and automatically generate optimized toolpaths, ensuring consistent quality, fast processing, and minimal material waste.

Our project follows a similar principle, but with a different workflow and application. Instead of relying on digital design files and specialized software, the cutting path is physically drawn directly onto the fabric. Our system will interpret these hand-drawn lines and guide the laser accordingly, eliminating the need for intermediate design software. This makes the process more intuitive, accessible, and adaptable.

2.2.4 Wattsan 6090 LT [4]

The Wattsan 6090 LT is a versatile laser engraver and cutter designed for precise work across a medium-format area, using an XYZ gantry system. It relies on digital design files that are transferred by software and processed by its controller. This allows the laser to follow exact paths for cutting a variety of materials.

Like that laser system, our project is based on this same principle, but the design input takes a different form. Instead of software-controlled paths, our system locates hand-drawn markings directly on fabric. This approach combines the precision of gantry-based laser cutting with the creative freedom of drawing patterns physically, rather than needing to generate them digitally.

2.2.5 APALES – Senior Design Group 5, Fall 2023 to Spring 2024 [5]

This past Senior Design project by UCF students named "Automated Parameter Adjusting Laser Engraving System" serves as an example of what we seek to build. This project used specific laser power and scan speed for each distinct material to be engraved. Each unique material was identified by a spectrometer, and the laser's power and speed were adjusted to operate on that material. Shapes could be engraved, but also a particular image could be uploaded to an application to have that engraved.

Our laser system will require more power because we will cut through certain fabrics instead of merely engraving them. Our project will have presets for the distinct parameters of varying materials. Similarly, thinking about safety, we will incorporate a fume extraction system to handle toxic fumes.

2.3 Project Goals & Objectives

2.3.1 Goals

- Basic goals
    - Laser beam cuts through fabric with kerf size of less than .5 millimeters
    - Beam from the laser diode is delivered to mirrors safely, and later the fabric
    - Human Machine Interface (HMI) boots with a functional, intuitive user interface
    - HMI clearly display operational options and system status
    - HMI clearly display job progress
    - Touchscreen shall be secure through a rigid panel mount that prevents loosening or flex
    - Touchscreen boots directly into a functional user interface without manual login or terminal interaction
    - Touchscreen options are clear and understandble to the user
- Advanced goals
    - Beam is expanded by >4x before reaching mirrors
    - Focused .1-.15mm diameter spot size using a four-lens system: 3 lenses and 2 prisms before the mirrors and one after
    - Collimated beam before contacting mirrors
    - HMI displays real time job preview from the camera
    - HMI displays descriptive error messages for user diagnostic
    - Include buzzer or speaker for events such as job completion or system errors
    - Store library of default or frequently used cutting jobs in internal storage
- Stretch goals
    - Sensor system integration that can identify reflectance and corresponding required passes for the fabric
    - Adjust power to account for different types of fabrics
    - Support job file upload via USB or wireless transfer
    - Log previous job parameters and error history for diagnostics
    - Integrate with a companion app for remote job upload and monitoring

2.3.2 Objectives

- Basic
    - Laser diode driver distributes current of 2.1A to laser diode, not reaching 3A operating current

    - Anamorphic prism pair corrects beam shape from elliptical to circular
    - The touchscreen shall withstand normal push force akin to the force a user would normally apply during normal operation
        - Under a typical finger press, visible bezel/frame motion shall be $\leq$0.2 mm
    - The Raspberry Pi Display 2 shall boot and launch the laser-cutter UI automatically through a kiosk-mode configuration within 30 seconds of powering on and will be fully interactable
    - Design the touchscreen UI layout with clearly labelled icons, consistent color coding, and font sizes
        - Conduct a user test with at least 3 people outside of the team. The interface passes if each person can correctly and confidently use the UI without external aid
- Advanced
    - Galilean beam expander expands beam by a factor greater than 7 prior to contact with mirrors
    - Display live job preview or camera feed for alignment verification
    - Log system faults automatically to system's internal storage in a first in first out manner based on available storage
    - Recall default jobs or material presets from internal storage without the need of any markings
    - Implement and onboard buzzer or speaker to provide audible feedback for key system notices such as job completion, errors, and emergency stops
        - Generate distinct audible tones for at least 3 system events (job completion, errors, emergency stop)
        - Ensure that each signal is audible at $\geq$70 dB some distance from the enclosure
        - Response latency $\leq$ 200ms between event trigger and audio activation
    - Implement color coded and descriptive error messages that specify the fault type (overheating, UART faults, visual loss from camera) and provide recovery instructions
        - Simulate 3 distinct error conditions and confirm that each generate a message within 1s of detection and remains visible until acknowledged by the user
    - Implement automatic restart of the system's UI if the OS crashes, ensuring continuous operation without user intervention
    - Display real-time job progression on the touchscreen through dynamic progress bars, numeric representation, or elapsed time indicators with estimated time to completion indicator
        - During testing, observe that the interface updates job completion metrics every $\leq$2s while the laser is active
- Stretch
    - Wireless job upload and download system that allows users to share G-code or job metadata via a companion mobile or web application

        - Demonstrate successful upload of a job file ≤ 1MB from the laser system to the app, and successful download and transfer of that same file to a second device over Wi-Fi or Bluetooth, with total transfer latency of ≤ 2s
    - Develop app functionality that allows a user to remotely monitor active jobs, system status, and error alerts in real time through a Wi-Fi or Bluetooth connection
        - App shall display live job progression, elapsed time, and system state (idle, running, or error) updated at ≤ 2s intervals. Information such as laser power and estimated time to completion will also be shown
        - App shall generate push notifications for any critical errors within ≤ 3s of detection
        - Connection shall remain stable for at least 10 minutes
    - Enable the onboard microcontroller (Raspberry Pi Pico 2) to receive and execute downloadable G-code jobs transmitted from the main Raspberry Pi 4B via UART or USB
        - Confirm end-to-end data transfer integrity by verifying that at least 99% of the data sent from the Pi 4B are received by the Pico 2 without corruption and that downloaded jobs execute identically to local jobs
    - Implement an onboard data logging system that records job metadata (duration, laser power, material type, completion status) and all system errors
        - Log entries shall include timestamp, job ID, and error code fields
        - System shall maintain a minimum of 50 records in local storage without corruption. Which a replacement system of first in first out
        - Logged data shall be exportable as a .txt file

2.4 Features & Functionalities

2.4.1 Optical Systems Diagram

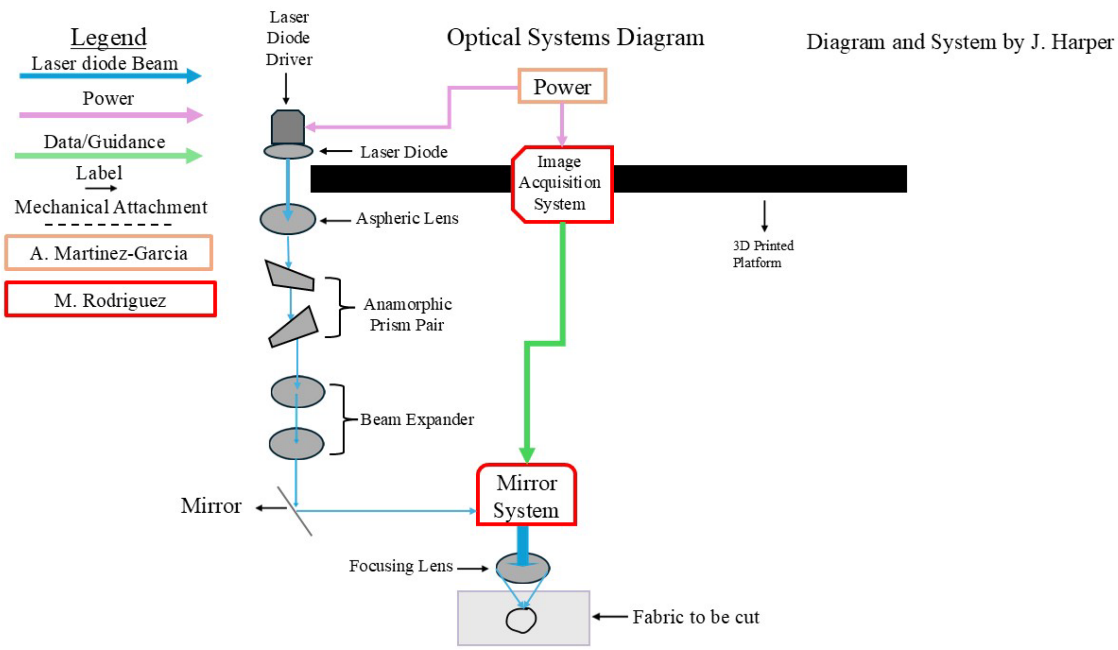

Figure 1: Optical Systems Diagram

The laser diode system shown in Figure 1 uses an anamorphic prism pair and three lenses, all secured by 3D printed mounts, to keep the laser diode beam collimated and enlarged as it approaches the mirror guidance system with the focusing lens. Collimation of the beam is essential because it minimizes divergence, or widening, of the beam as it travels. The initial lens of the system is aspheric, which will collimate the beam into the anamorphic prism pair that corrects the beam shape. Followed by the beam expander system composed of two lenses, expanding the beam size incident on the mirrors. The beam expander in this system ensures the beam spot size on fabric will be small because the beam incident on the focusing lens is large.

To move the mirrors and redirect the laser beam onto any specific spot of the fabric canvas the user desires to cut, there are two viable mechanisms that were investigated: a moving gantry and galvo motor system. Both mechanisms quickly and efficiently direct the beam and have their advantages and disadvantages.

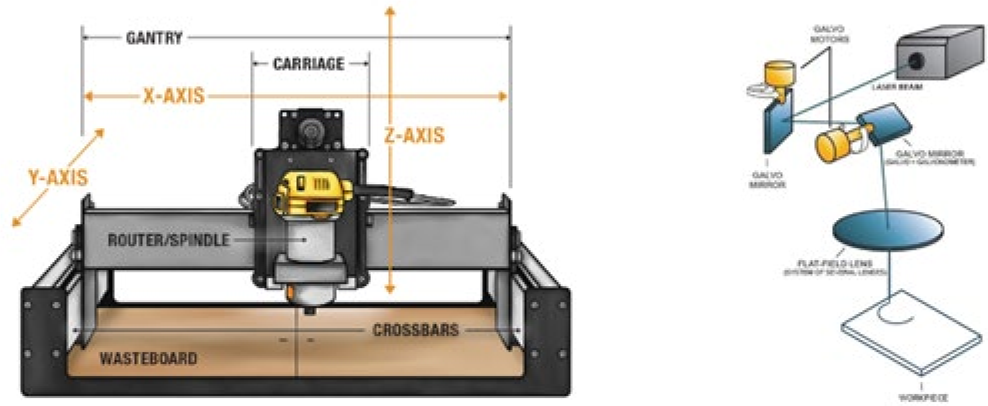

Figure 2: Illustrations of the galvanometer system [23,24]

A galvanometer system uses two small fast-moving mirrors mounted onto galvo motors to precisely control the direction of a laser beam onto a specific point on a two-dimensional plane. By rotating the motors with electric signals, the angle of the mirrors change, and the direction of the reflected laser beam changes. The mirrors are used together, one for the x-axis and one for the y-axis. This system works quickly and precisely to rapidly move a laser on a 2D plane, needing very few mechanical parts and with a very compact design. To make sure the beam is focused at the same spot size and reduce distortion on the edges of the field, an f-theta lens is used after the mirrors.

This system is much superior to moving gantry systems on small fields, but as field sizes increase, the galvanometer system becomes a lot less practical. This system has a limited scanning angle. Since the size of the mirrors limits the max scanning angle, larger mirrors would be required to prevent the laser from clipping. The entire 350 mm x 350 mm field may not be accessible to the system in the confined space of the enclosure. The light entering an f-theta lens is usually between 15 to 20 degrees, and no larger than 28 degrees. [25, 26] Based on the area of the field, the focal length of the desired f-theta-lens can be determined:

$$\frac{350}{2\tan(\theta)} = f$$

Even at the maximum angle, the required focal length is 330 mm, which is very large. In fact, none of the f-theta lenses available on Thorlabs or Edmund Optics can cover the entire field except for one; with a focal length of 650 mm and a scan angle of 24 degrees, it could cover a maximum field area of 410 mm x 410 mm. There are only two downsides, the wavelength range is near infrared, and the cost for a single lens is over seven thousand dollars. [25, 26]

A moving gantry system would be much more practical and economical for this field size since it can be scaled up for larger areas without requiring larger optics but instead just scaling the beam sizes to the size of the field area.

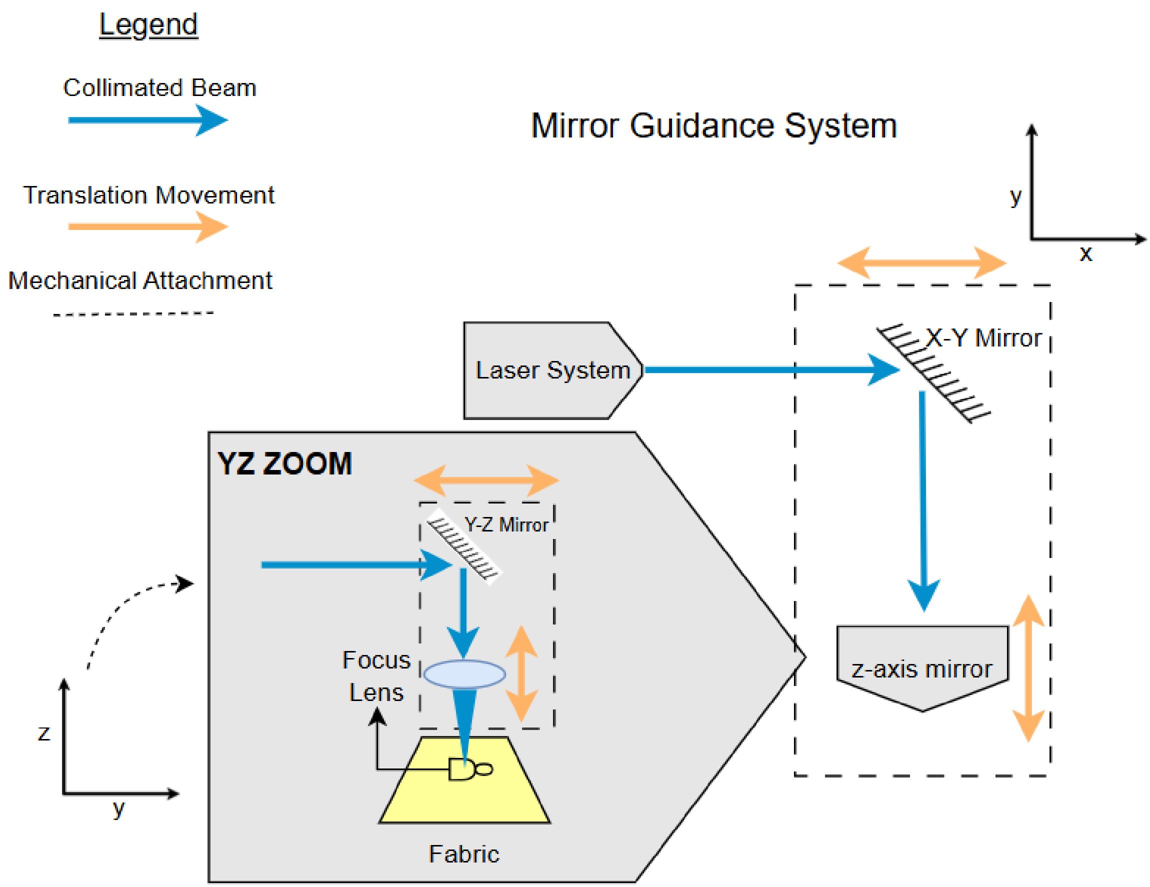

Figure 3: Beam Guidance System Diagram

To best guide this beam with the least amount of divergence and distortion possible, a moving XY gantry mirror system (Figure 2) will be implemented for scanning the entire 350 x 350 mm field. Both mirrors will move in the x-direction together on a shiftable crane component above the fabric, dictating the x-position of the beam. A second downward-facing mirror will move independently in the y-direction along the crane component itself, dictating the y-position of the beam and directing the beam onto the fabric. This makes it possible for the beam to reach any x-y position on the fabric canvas.

At this stage, the beam is still large and collimated with low intensity. Mounted on the same unit as the second mirror, directly under it, is a convex lens to focus this beam to get the final small beam spot and high optical intensity on the desired line to be cut. Since the thickness of the fabrics may differ, the focus lens will be able to translate up and down in the z-direction, ensuring uniform focus spot of high intensity and high precision cutting on a multitude of fabrics.

To be able to detect and locate the lines, a camera mounted overhead will capture an image of the entire fabric canvas in bright ambient lighting before the job is initiated. To avoid distortion at the edges of the image, a narrow FOV camera will be used over a foot above the fabric. Once the image is captured, it is analyzed, the lines are confidently discerned from the fabric, and the pixels will be mapped into coordinates for the beam guiding system to follow.

2.4.2 Subsystem Features

- Laser Diode System
  - Laser Diode (LD)
    - Beam exiting diode is elliptical and diverges as it travels
    - Beam from LD is guided by mirror system to burn/cut through textiles
  - Laser Diode Driver
    - Delivers constant current to LD, staying below max current threshold of 3A
    - Delivers operating voltage to LD, staying below the maximum voltage value of 5.2 and ensuring a reverse voltage of 2 volts.
  - Lens System
    - Aspheric lens focuses beam into the anamorphic prism pair that corrects the beam shape meaning the slow (horizontal) and fast (vertical) axis of the beam exiting the laser diode
    - Dual lens beam expander system enlarges beam before contacting mirrors with focusing lens
- Beam Guiding System
  - Plane mirrors
    - Mirrors fixed at 45° angle with respect to the beam for redirection in each axis
    - Reflect >99% of the incoming beam
  - Gantry rail/motors
    - Smooth precise movement of mirrors
  - Focus lens
    - Maximizes beam intensity on fabric
    - Adjustable height to compensate for fabric thickness
- Image Acquisition System
  - Camera
    - Capture entire fabric canvas area
    - Minimal/no edge distortion
    - Capture high quality images
  - Image processing
    - Reliably contrast/filter lines from the rest of the fabric, if not then error
    - Convert line pixels into gantry coordinates with <1% error
  - Ambient lighting
    - Steady ambient lighting during image capture
- Touchscreen
  - Interactive User Interface
    - 7” multi-touch capacitive touchscreen with intuitive menu navigation

        - Large buttons/Icons to avoid unintended actions
    - Job Management
        - Upload job files via USB flash drive (stretch)
        - Display job preview before starting
        - Select from default jobs integrated into the machine (advanced)
        - Select from stored jobs previously used that were uploaded into the machine
    - Cutting Controls
        - Start, pause, resume, and stop a job from the screen
        - Adjust laser speed and power
    - Status Feedback
        - Real-time progress display to show percent completed and estimated time remaining
        - Descriptive error messages
        - Indicators of the current state of the machine (running, idle, error)
        - Audio feedback via buzzer or speaker
    - Safety
        - Automatic stop when errors occur
        - Emergency stop button

2.5 Component Specifications

Table 1: Component Specifications

Component	Parameter	Specification	Unit
Housing			
Honeycomb Base	a) Dimensions b) Thickness	a) 400 x 400 b) 22	a) Millimeters b) Millimeters
System Housing	Dimensions	600 x 600 x 600	Millimeters
Camera	Height	441	Millimeters
Laser Diode System			
Laser Diode	a) Wavelength b) Optical Power Output c) Beam Diameter d)Threshold Current e) Operating Voltage f) Operating Current	a) 445-465 b) 3500 c) TBD d) .25 - .3 e) 4.4-5.2 f) 3 g) 0-60	a) Nanometers b) Milliwatts c) TBD d) Amps e) Volts f) Amps g) Celsius

	g) Operating Temperature		
Laser Diode Driver	a) Current Delivered b) Max Voltage c) Operating Temperature	a) TBD b) TBD c) TBD	a) Amps b) Volts c) Celsius
Aspheric Lens (Thorlabs-C140TMD-A)	a) Focal Length b) Diameter c) Coating d) Diameter with Mount	a) 1.5 b) 2.4 c) ThorlabsA: 300-750 d) 6.2	a) Millimeters b) Millimeters c) Nanometers d) Millimeters
Anamorphic Prism Pair (Thorlabs-PS873-A)	a) Focal Length b) Size c) Coating d) Diameter with Mount	a) N/A b) < 12x12 c) Thorlabs ARC: 350-700	a) N/A b) Millimeters c) Nanometers
Plano-Concave Lens (Thorlabs-LC1975)	a) Focal Length b) Diameter c) Coating	a) -23.9 b) 6 c) Uncoated	a) Millimeters b) Millimeters c) N/A
Bi-Convex Lens (Thorlabs- LB1945-AB)	a) Focal Length b) Diameter c) Coating d) Exiting Beam Diameter	a) 200 b) 1 c)Thorlabs A: 300-750 d) 1.32	a) Millimeters b) Inches c) Nanometers d) Millimeters
Mirror Guiding & Focusing System			
Mirror A	a) Reflectivity b) Diameter c) Wavelength	a) >99% b) 7 c) 400-750	a) N/A b) Millimeters c) Nanometers
Mirror B	a) Reflectivity b) Diameter c) Wavelength	a) >99% b) 7 c) 400-750	a) N/A b) Millimeters c) Nanometers
Focusing Lens	a) Focal Length b) Diameter c) Coating	a) 17.9 (at 455 nm) b) 6.5 c) AR	a) Millimeters b) Millimeters c) N/A

	d) Beam Size	d) TBD	d) TBD
Camera-Tracking System			
Camera	a) Resolution b) Field of View c) Shutter Speed d) Aperture	a) 1920×1080 b) ~40-60 c) 1/100 d) TBD	a) Pixels b) Degrees c) Seconds d) f/#
Touchscreen System			
Screen	a) Touch b) Brightness c) Input latency d) Resolution e) Viewing Angle f) Size	a) Five-touch capabilities b) ≥500 c) ≤100 d) 720 x 1280 e) ≥80 f) 7	a) Pressure Points b) Nits c) Milliseconds d) Pixels e) Degrees f) Inches
Controller/Processor	a) CPU Speed b) RAM c) Power Draw d) Boot Time	a) 1.5 b) 4 c) ~3.4 - 7 d) ~25	a) Gigahertz b) Gigabytes c) Watts d) Seconds
Storage	a) Type b) Size c) Read speed d) Write speed	a) High Endurance b) 256 c) 100 d) 40	a) Class b) GB c) Megabytes per second
Buzzer	a) Frequency b) Trigger Latency	a) 2000 - 4000 b) <1	a) Hertz b) Millisecond
Power System			
Power Supply	a) Efficiency b) Load Regulation	a) ≥74 b) ≤8	a) Percentage b) Percentage

Table 2: Engineering and Performance Specifications

Engineering Requirement	Requirement Specification	Unit

Housing System		
Camera Height	463	Millimeters
		Millimeters
Laser Diode System		
Laser Diode Max Output Power	3.5	Watts
Max voltage delivered to LD	<5.2	Volts
Beam size incident on mirrors	<7	Millimeters
Beam Guiding System		
Mirrors direct laser beam	>10	Millimeters per second
Reflectivity	>99	Percent
Speed		
Image Acquisition System		
Sensor resolution	4608 × 2592	Pixels
Horizontal FOV	66	Degrees
Vertical FOV	41	Degrees
Depth of field	10 - ∞	Centimeters
Touchscreen System		
The system shall boot within and show the system UI within a reasonable amount of time	≤30	Seconds
The system shall show clear images from the camera system and clearly show written text.	720 x 1280	Pixels

The system shall provide user feedback on errors and job progression	≥90% of errors produce an onscreen message	Percentage
The system shall provide audio feedback on job completion and errors	≥70	dB

2.6 Hardware Block Diagram

The figure below shows the hardware block diagram for the overall project design. The hardware block diagram involves three main subsystems: the power supply unit, the laser system and the printed circuit board (PCB). The power supply unit serves to provide and distribute stable power to all of the components. The laser system contains several components that will be instrumental in enabling the laser to cut fabrics. All of the subsystems work in tandem to deliver the final product. Each given part of the design is color-coded to establish who in the team will be responsible for that task.

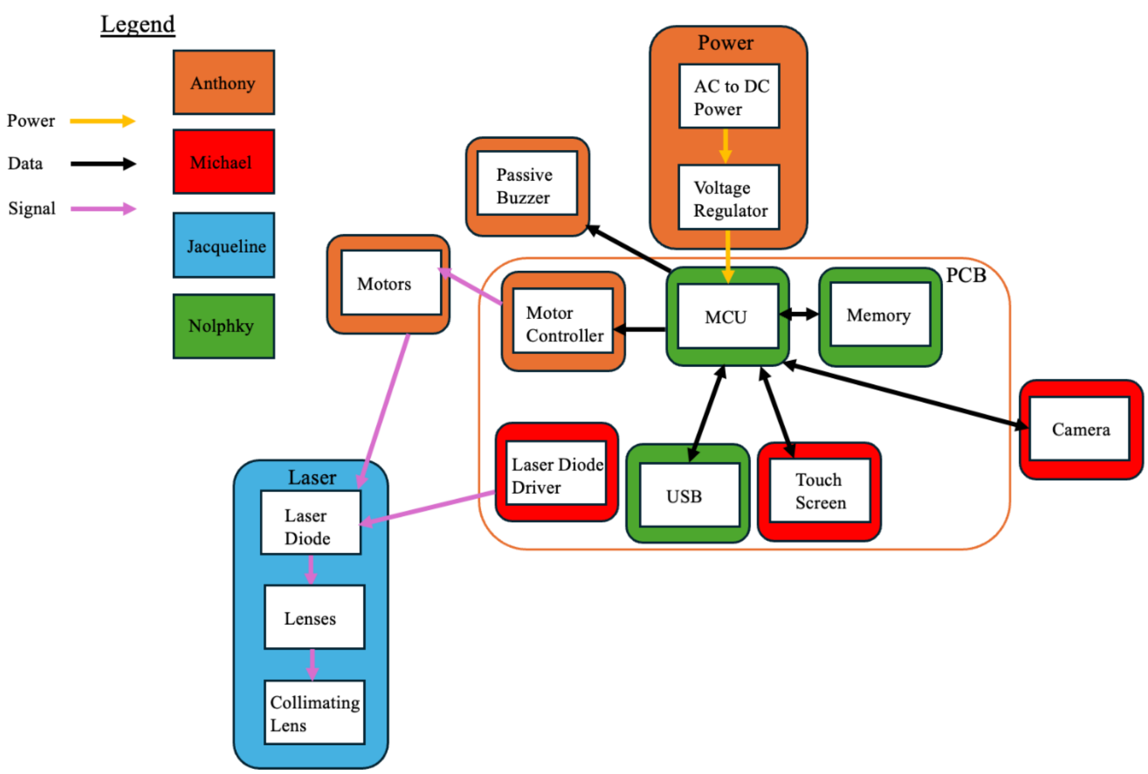

Figure 4: Hardware Block Diagram

2.7 Software Diagram

2.7.1 Touchscreen Flowchart & Description

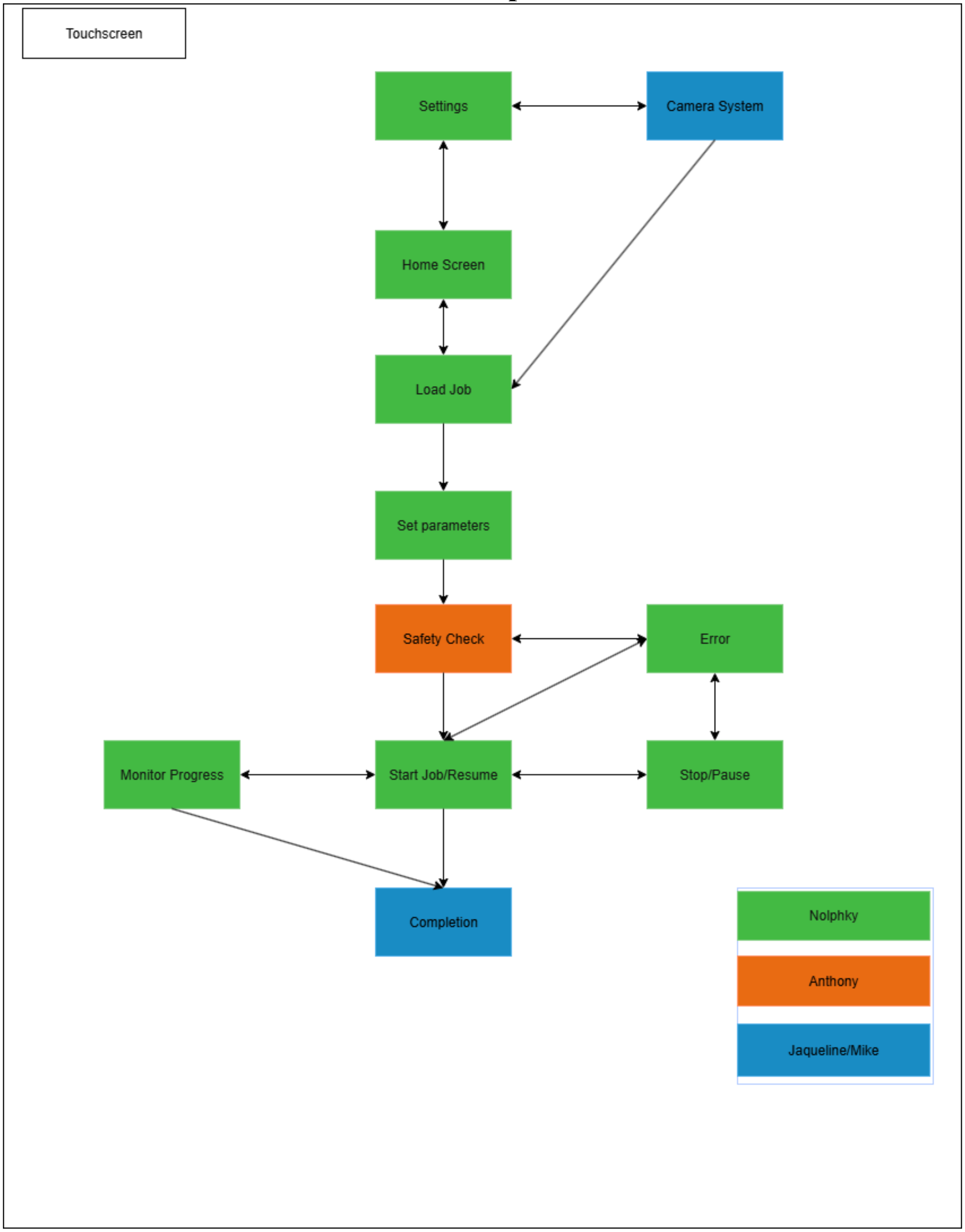

Figure 5: Touchscreen Flowchart

- **Home Screen**
    - Access Settings
        - Control over system preferences
        - Configure camera system (alignment, job preview, calibration)
        - Load job – Selects a cutting job from the camera system or, as a stretch goal, via USB drive or Bluetooth file transfer
- **Load Job**
    - Captured by the camera system (preview image available)
- **Set Parameters**
    - Allows for users to configure power, speed, and number of passes
    - Includes material presets for common fabrics
- **Safety Check**
    - The software verifies critical safety check
    - Any failures will lead to an error screen
- **Error Handling**
    - Displays descriptive warnings
    - Prevents the system from starting until conditions are corrected
- **Start Job/Resume**
    - Sends job parameters and cutting commands to the controller
    - Initializes job timer and enables real-time monitoring
- **Monitor Progress**
    - Displays percent completed, estimated time remaining, and live status
    - Emergency stop and pause options are also available on this screen
- **Stop/Pause**
    - User can halt or pause the cutter mid-operation
    - Software ensures the laser powers down safely
- **Completion**
    - Once a job is finished, a confirmation message is displayed. The software logs the job and returns the user to the home screen
    - Provides an option to review job statistics

2.8 Prototype Illustration/Blueprint

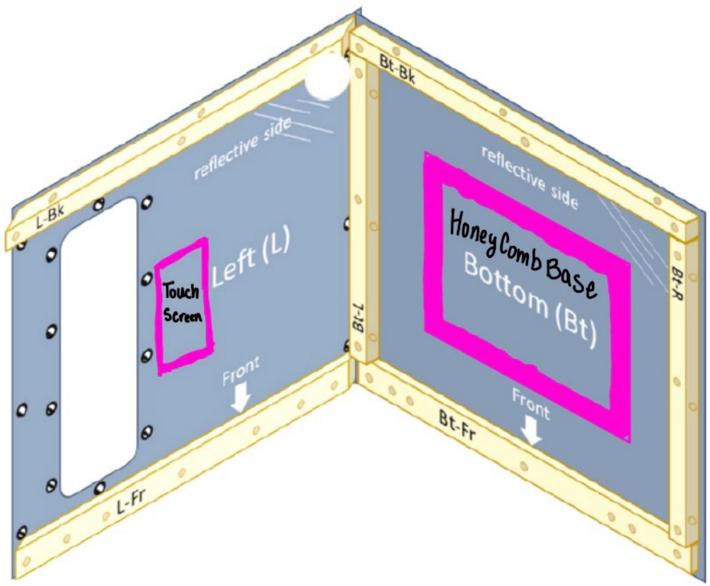

Figure 6: Partially Assembled Prototype with Touchscreen and Honeycomb Base

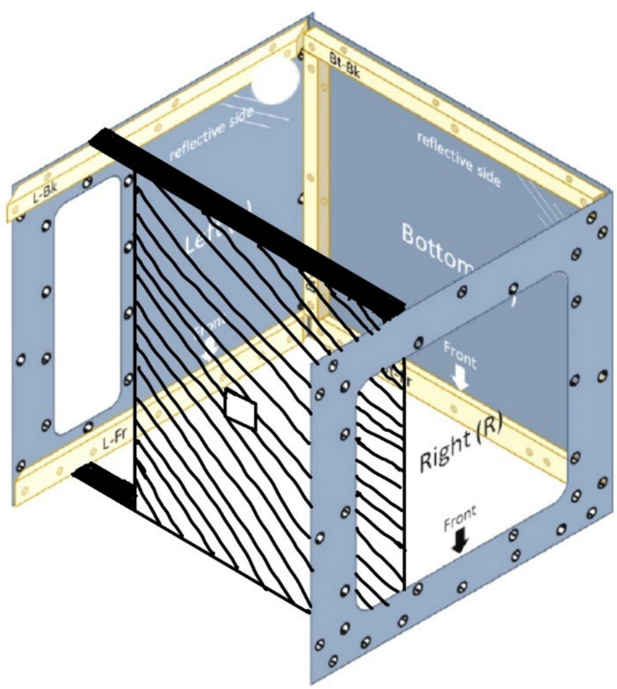

Figure 7: Partially Assembled Prototype with Platform

Since we are purchasing this enclosure, we know the size will be 600x600x600 mm. The enclosure is equipped with OD6+ laser safety windows instead of the clear windows shown in the figures above. This enclosure gives us space to secure each of our subsystems, protects our laser cutting area from outside forces, and gives us easy access to adjust these subsystems once the project is built. We will be utilizing the UCF manufacturing lab to cut extra space in the panel or side of the enclosure for our touchscreen and possible fan system.We will be placing a 400x400mm honeycomb base at the bottom of the cutting system so that there is minimal contact between the fabric and metal as the fabric is being cut by the laser. The honeycomb base and the touchscreen are shown in Figure 6. We will be constructing a 3D-printed platform to separate the gantry system from the power system and anything required to run the touchscreen and camera system. The power systems will be on top of this platform and it will have a space cut so that the optical system rail can be on one side of the enclosure pointing down, with the laser diode above the platform and beam exiting below the platform. There will be a hole-like notch to fit the camera and hold it in place at the height needed to view the entire honeycomb base, shown in Figure 7.

2.9 House of Quality

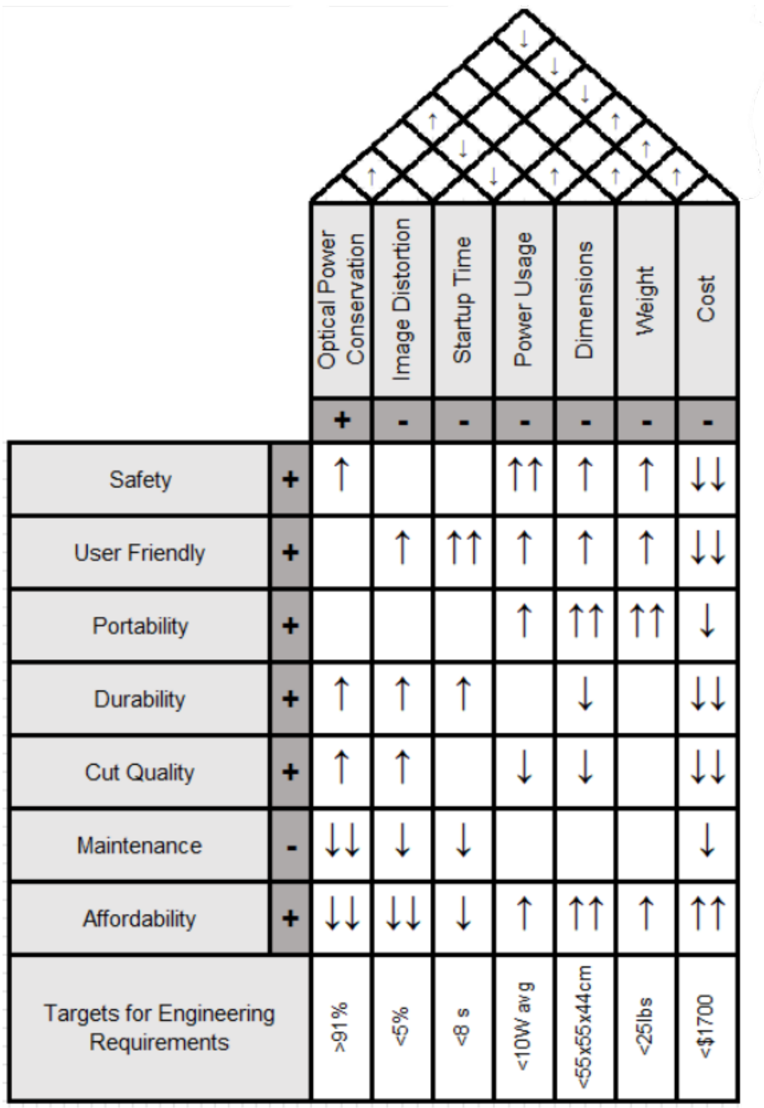

Figure 8: House of Quality

2.10 System Architecture Overview

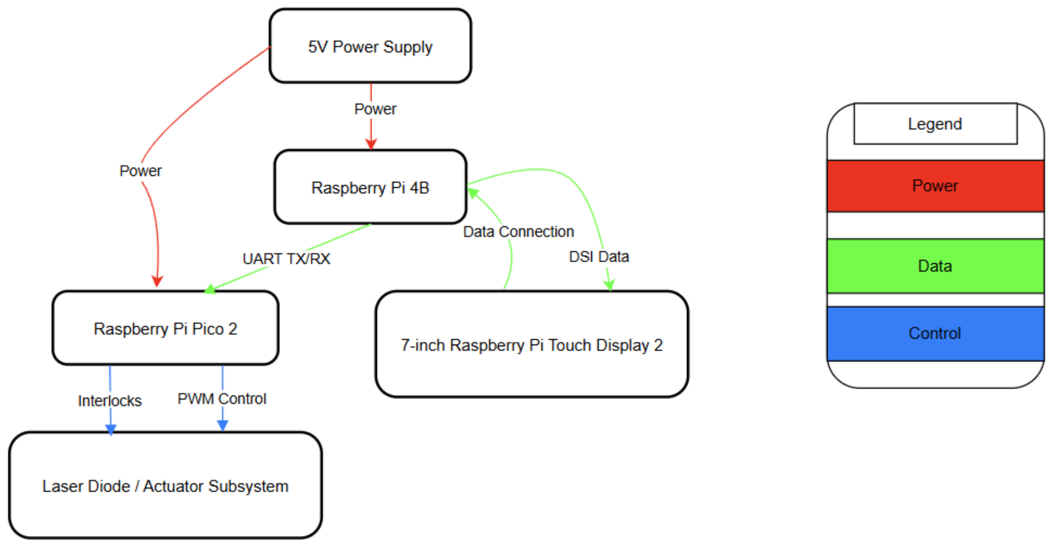

Figure 9: System Architecture

The architecture of the Fabric Laser Cutter System (F.L.C.S.) is organized into a two-tier control structure that separates user interaction from real-time process control. As shown in Figure 9, the Raspberry Pi 4 Model B serves as the supervisory controller and hosts the graphical user interface displayed on the 7-inch Raspberry Pi Touch Display 2 through a direct MIPI-DSI ribbon connection. This computer handles high-level functions such as job loading, parameter configuration, and monitoring system status. It communicates with the Raspberry Pi Pico 2 microcontroller, which operates as a dedicated real-time controller responsible for laser pulse-width modulation, safety interlocks, and emergency shutdown handling. The 5 V power supply distributes regulated voltage to both controllers and peripheral circuits, ensuring stable operation. Control and feedback signals link the Pico 2 to the laser diode and actuator subsystem, enabling deterministic laser firing while maintaining user-level control from the graphical interface. This modular design improves safety, reliability, and maintainability by isolating high-latency user processes from time-critical laser control logic.

Chapter 3: Research

3.1 Hardware Research

3.1.1 Housing Comparison Table & Description

Table 3: Housing Comparison Table

Enclosure/Housing

Name or Product (Brand)	Laser Engraver Cover (Creality)	Professor Laser Engraver Enclosure (Makergadgets)	Innovator 3D Printer/Engraver Enclosure (Makergadgets)
Material	Flame-retardant fabric	Aluminum	Aluminum
Dimensions (mm)	700x720x400	724x699x292	600x600x600
Acrylic Window Dimensions (mm)	255x255	200x600	(2) 216x356
Additional Features	Zipper, lightweight, OD6+ viewing window, Hinged door on top	Door on top, OD6+ viewing window	Hinged side door, OD6+ viewing window
Cost (USD)	59.99	Originally 99.99, 125.00 with OD6+ window	99.99 base price, up to 180.00

When considering how to build our housing, this group was limited due to the absence of a mechanical engineer. To avoid mistakes in designing the main structure for our system, we opted to purchase an enclosure to house our system. After noticing the fabric material used in the Creality Laser Engraver Cover, we decided to focus our efforts on finding housing that would be an affordable metal such as aluminum. This was done to eliminate concerns when using flammable materials. By filtering our scope based on our desired material we were able to limit our other options to two enclosures offered by Makergadgets.

Between our available options, we prefer the "Innovator", this enclosure has a side door that will allow us to mount the camera and laser diode module towards the top of the interior, staying stationary, while allowing the user to open and close the door as needed and easily view the cutting system at work. These Makergadgets brand options are larger than our initial dimensions, but this extra space will be taken up by necessary electronic components, the mirror and focusing guidance system, as well as stabilizing components to ensure movement of our guidance system does not move the fabric. The "Innovator" comes equipped with a two-phase air purification system that absorbs harmful compounds and fumes using high efficiency particulate air filters or HEPA filters. These types of filters have been confirmed by NASA as well as the University of Minnesota to remove 99.99% of nanometer-sized particulates [6]. For this enclosure to be the most practical, we will be cutting out some of the aluminum to make space for our touchscreen and possible supplemental fan system. We will be cutting this aluminum using the manufacturing lab at UCF.

3.1.2 Touchscreen Comparison Table & Description

Table 4: Touchscreen Comparison Table

	Raspberry Pi Touch Display 2 (7”)		**Generic 7” HDMI touchscreen**	**10.1” HDMI Touchscreen**
Resolution	720x1280		1024x600	1280x800
Size	7”		7”	10.1”
Touch Spec	Capacitive (5-point)		Capacitive (5-10 point)	Capacitive (5-10 point)
Connection to Pi	DSI ribbon (video) + 5 V GPIO (power/touch)	HDMI (video) + USB (touch) + 5 V barrel/USB (power)	HDMI (video) + USB (touch) + 5 V barrel/USB (power)	
Driver Support	Native in Raspberry Pi OS, no config needed	USB HID (works as generic mouse) usually plug & play	USB HID (works as generic mouse) usually plug & play	
Cable Management	Very clean (only ribbon + jumper)	Messy (HDMI + USB + power cable)	Messy (HDMI + USB + power cable)	
Power Draw	~2.4-3 W	~3-5W	~5-8W	
Ease of Mounting	Panel mount, slim	Often thicker, may need custom bezel	Bulkier, needs larger cutout	
UI Real Estate	Limited (good for menus and buttons)	More space for menus/status	More space; can show job preview or even webcam feed	
Cost	~$80	~40-70	~$80-130	
Best for	Clean integration, guaranteed	Slightly higher resolution on same footprint	Larger UX, multi-window layouts, more “industrial” look	

	support, low hassle		
Link	Raspberry Pi Touch Display 2	$48 Amazon $42 elecrow $44 waveshare	Amazon link around $84

Three candidate touchscreen options were considered: the Raspberry Pi Touch Display 2, a set of generic 7-inch HDMI panels (such as the Waveshare and Elecrow 1024x600 models), and a 10.1-inch HDMI touchscreen (such as the ROADOM 1280x800 display). The HDMI panels provide slightly higher resolution than the official Pi display, with the 10.1-inch screen offering more UI real estate for previews and menus. However, both HDMI options require multiple connections (HDMI for video, USB for touch, and separate 5 V power), which complicates cable management inside the enclosure and introduces potential signal interference if cables are unshielded[7][8].

In contrast, the Raspberry Pi Touch Display 2 uses a native MIPI-DSI ribbon for video and draws power directly from the Pi's GPIO header, yielding a compact, lightweight assembly with minimal cable clutter[9]. This tight integration also reduces potential mechanical strain on connectors and improves long-term reliability in an enclosed system where space is limited. Because the official display is supported natively within Raspberry Pi OS, no external USB drivers or calibration utilities are required, ensuring plug-and-play operation and long-term maintainability[10].

Long-term reliability is a nice addition that comes with the touch display 2. Since it is produced and supported by Raspberry Pi Ltd., its drivers are bundled directly within official Raspberry Pi OS releases. This ensures continued compatibility with future kernel updates and firmware revisions without requiring external configuration or third-party patches.

From a thermal and power perspective, the official display is also advantageous. Drawing power directly from the Pi's regulated 5 V rail ensures stable voltage levels and avoids the potential ground loops or noise that can occur with separate HDMI and USB power lines. With a measured draw of approximately 2.5 W during normal operation[11], it contributes less heat to the enclosure and maintains overall system efficiency, which is an important factor in a closed laser-cutter chassis where airflow is limited.

The DSI connection also reduces electromagnetic interference within the control enclosure. HDMI and USB cabling can act as radiating loops (especially when unshielded) that introduce signal noise into nearby low-voltage PWM and sensor lines. The MIPI-DSI ribbon uses short, low-voltage differential pairs that minimize radiated emissions and susceptibility to noise, which is advantageous in systems involving precision laser timing and analog sensing.

From an ergonomic standpoint, a 7-inch display size provides sufficient screen space for large, easily navigable icons and menus without taking too much space on the available front-panel dimensions of the enclosure. A higher resolution 10.1-inch screen is visually appealing but is not necessary and conflicts with the system's compact form factor.

Finally, extensive community forums and official resources further supported the choice to use the Raspberry Pi Display 2 over the others. Because it is part of the Raspberry Pi's ecosystem, guides, libraries, and troubleshooting information are available through documentation and developer forums. This greatly reduces potential integration issues and lowers development time compared to lesser-known third-party HDMI panels.

3.1.3 Controller Comparison Table & Description

Table 5: Touchscreen Controller Comparison Table

	Raspberry Pi 4B	**Raspberry Pi 5**	**Arduino Mega 2560 Rev3**	**NVIDIA Jetson Nano**	**ESP32-WROOM**
Ram	4GB LPDDR4 SDRAM	LPDDR4X-4267 SDRAM 4GB	8kb SRAM	4GB 64-bit LPDDR4 25.6GB/s	520 KB SRAM, 4 MB Flash
Processor	Broadcom BCM2711, quad-core Cortex-A72 (ARM v8) 64-bit SoC @ 1.5GHz	Quad-core 2.4 GHz Arm Cortex-A76	ATmega2560	Quad-core ARM® Cortex®-A57 MPCore	two low-power Xtensa®32-bit LX6 microp

				processor @ 1.43GHz	rocessors
Graphics/Display	VideoCore VI 3D Graphics	Video Core VII	none	128-core NVIDIA Maxwell™ architecture GPU	none
Connectivity	2.4 GHz and 5.0 GHz IEEE 802.11b/g/n/ac wireless LAN, Bluetooth 5.0, BLE Gigabit Ethernet 2 × USB 3.0 ports 2 × USB 2.0 ports	2.4 GHz and 5.0 GHz IEEE 802.11 b/g/n/ac wireless Bluetooth 5.0, BLE Gigabit Ethernet 2 × USB	54 digital I/O pins 4 hardware UARTS USB B connector	Gigabit Ethernet 4 x USB 3.0 ports Micro USB/USB C HDMI 2.0 Display port	Wi-Fi 802.11 Bluetooth v4.2 BR/EDR and BLE specification NZIF receiver with –97 dBm sensitivity SD card,

					3.0 ports 2 × USB 2.0 ports			UART, SPI, SDIO, I2C, LED PWM, Motor PWM, I2S, IR, pulse counter, GPIO, capacitive touch sensor, ADC, DAC
Cost	$59.99				$60.00	$49.90	$129.00	
Power Requirement	5V 3A (USB-C power supply)	5v 5A (USB-C power supply)	5V 7V-12V (recommended input)	5V	3V - 3.6V			
Operating Temperature	0–50ºC	0–50ºC	–40 °C ~+85 °C	–25 °C ~+85 °C	–40 °C ~+85 °C			

In evaluating potential controllers for this project, five options were considered: the Raspberry Pi 5, Raspberry Pi 4B, Arduino Mega 2560, and ESP32-WROOM. The Arduino Mega 2560, while inexpensive and reliable for low-level embedded control, lacks an operating system, GPU, and sufficient memory, making it unsuitable for a system requiring a touchscreen interface. Similarly, the ESP32-WROOM, recommended by a peer for its strong bluetooth and WI-FI capabilities and ease of programming through the CP2102 USB-to-UART bridge, excels in IoT and wireless applications but falls short in onboard computing power, GPU support, and OS capabilities. It is better suited for real-time, low-level control, whereas this subsystem requires a supervisory-level controller capable of running a graphical interface and managing multiple software processes.

The Jetson Nano offers significant graphical and AI-processing performance, but its higher cost, greater power consumption, and lack of onboard wireless connectivity would add unnecessary complexity, particularly if the project's stretch goal of Bluetooth communication is pursued. Between the two Raspberry Pi options, the Pi 4B provides a proven balance of cost, community support, and performance, while the pi 5 offers improved CPU and GPU resources and higher RAM options, making it a more future-proof choice. Ultimately, the Raspberry Pi family was selected as the most suitable controller platform due to its ability to run a full Linux operating system, support a native touchscreen interface, and balance affordability with the required computational capabilities. Between the two, however, the Pi 4B is chosen because it requires a smaller power supply, has lower cost, and is more field proven than the newer Pi 5.

3.1.4 Microcontroller Comparison Table & Description

Table 6: Microcontroller Comparison Table

Microcontroller	**Process/ clock**	**Key Features**	**Pros**	**Cons**	**Fit for project**
Raspberry Pi Pico 2	Dual-core ARM Cortex-M33 @ 150 MHz	520 KB on-chip SRAM USB drag and drop programming	• Excellent timing precision (< 1 µs interrupt latency) • Low cost (< $10) • Easy USB programming • Strong	• Limited flash/RAM • No RTOS (bare-metal or simple scheduler)	**Selected** – provides reliable real-time control for laser PWM and safety interlocks

			community and Raspberry Pi integration		
Arduino Mega 2560	8-bit AVR @ 16 MHz	54 GPIO, UART, SPI, I²C	• Widely used and beginner-friendly • Excellent Arduino library support	• 8-bit MCU with limited speed; not ideal for precise timing or heavy serial traffic	Slower; insufficient timing resolution for laser PWM
STM32 F4 Series	32-bit ARM Cortex-M4 @ 180 MHz	Advanced timers, DMA, RTOS support	• High-performance MCU with rich peripherals • Can run FreeRTOS for multitasking	• Higher cost • Requires more complex toolchain and setup	Viable but adds unnecessary complexity for a student project
ESP32-WROOM	Dual-core Xtensa LX6 @ 240 MHz	Wi-Fi, Bluetooth, FreeRTOS support	High clock speed, wireless connectivity, low power	Nondeterministic timing due to background Wi-fi/Bluetooth tasks	Considered but not selected. Unsuitable for strict real-time laser control

After evaluating multiple microcontrollers such as the Arduino Mega 2560 and STM32 F4 Series, the team ultimately selected the Raspberry Pi Pico 2 for the real-time control layer. Compared to the Arduino Mega's slower 16 MHz clock speed, the Pico 2's dual-core ARM Cortex-M33 processor running at 150 MHz provides microsecond-level timing, ideal for laser PWM gating and safety interlocks. Using the fundamental clock-period equation

T=1/f, this corresponds to approximately 6.7 nanoseconds per cycle, demonstrating the Pico 2's capabilities to handle sub-microsecond interrupts with deterministic precision.

While the STM32 F4 Series offers even higher performance, it introduces greater cost and toolchain complexity than required for this project. The Pico 2 delivers a strong balance of performance, cost, and ecosystem support with 520 KB of on-chip SRAM, simple USB drag-and-drop programming, and full compatibility with the Raspberry Pi SDK. These factors make it a reliable and affordable choice for deterministic real-time control without adding unnecessary complexity to the overall system.

The ESP32-WROOM was also briefly considered for this layer due to its dual-core architecture and integrated Wi-Fi and Bluetooth connectivity. However, its background wireless stacks and FreeRTOS scheduling introduce nondeterministic timing, making it less ideal for precise PWM control and interrupt-based safety interlocks. It remains a viable option for future versions that may require wireless diagnostics or distributed subsystems, and its low cost allows it to be acquired for testing or prototype experimentation if needed.

3.1.5 Communication Interface Selection

Table 7: Communication Interface Table

Interface	**Typical Speed**	**Wiring Complexity**	**Processor Overhead**	**Determinism**	**Debugging Ease**	**Fit for project**
UART	Up to ~1 Mbps	2 lines (TX/RX)	Low	High	Excellent (serial monitor)	Chosen: reliable, low-latency control link
SPI	Up to ~10 Mbps	4 lines + CS (with more peripherals)	Moderate	High	Moderate (logic analyzer)	High speed but requires more pins

I²C	Up to 400 kbps	2 lines (SDA/SCL)	Moderate	Medium (shared bus)	Difficult (shared addressing)	Simpler wiring but less robust timing
USB	12 Mbps (Full) / 480 Mbps (High)	2 differential pairs	High (stack driver)	Low	Complex (driver-dependent)	Good for firmware update & power, not for real-time link

Several communication interfaces were evaluated to connect the Raspberry Pi 4B supervisory computer with the Raspberry Pi Pico 2 real-time controller. The selection process considered bandwidth, wiring complexity, processor overhead, determinism, and ease of debugging. Table 7 summarizes these tradeoffs among common embedded communication standards.

Based on these criteria, UART was selected as the primary control-link protocol for the F.L.C.S., balancing reliability, simplicity, and real-time responsiveness. Its minimal wiring and low CPU overhead reduce integration effort, while its compatibility with standard serial-monitor tools (such as PuTTY, minicom, or the Arduino Serial Monitor) allows us to easily observe and troubleshoot communication during testing and maintenance. This combination of practical debugging visibility and deterministic timing makes UART the most suitable interface for ensuring stable coordination between the two controllers.

3.1.6 Timing Budget and Determinism Requirements

In real-time embedded systems, each subsystem operates under different latency and determinism requirements. Human-interface actions, such as touchscreen input or menu updates, can tolerate delays in the order of tens of milliseconds without affecting usability, while laser gating and motion control demand precise, repeatable timing at the microsecond scale. To formalize these expectations, a timing budget was established to define acceptable response times and jitter for major operations within the F.L.C.S. architecture. The values in Table 3.X are derived from standard practices in motion-control and laser-marking systems, emphasizing deterministic execution for safety-critical tasks while allowing non-real-time flexibility for high-level functions handled by the Raspberry Pi 4B. This breakdown clarifies why timing-sensitive operations are delegated to the Raspberry Pi Pico 2, ensuring consistent laser performance and rapid fault response.

Table 8: Timing Budget Table

Operation Type	**Example Task**	**Target Latency (max)**	**Allowable Jitter**	**Runs On**	**Rationale**
Image Processing /Job Preparation	Convert imported image to toolpath or raster data; generate G-code	>100 ms	N/A	Pi 4B (Linux)	Heavy computation. Not real-time and timing not critical to safety or control
UI/HMI	Touch press. Button highlight; screen refresh	≤ 100 ms	≤ 20 ms	Pi 4B (Linux)	Human-perceptible but tolerant
Job I/O & Logging	Load design, write CSV logs	10 - 100 ms	≥ 10 ms	Pi 4B (Linux)	Not real time
Command dispatch	Send motion/laser commands to MCU	≤ 2 ms (average)	≤ 0.5 ms	Pi 4B outgoing via UART	Smooth streaming to MCU
Step pulse generation	Step/dir for steppers	≤ 5 µs ISR service	≤ 2 µs	Pico 2	Prevent missed microsteps at high feed

Laser PWM gating	Modulate laser power	≤ 10 µs edge timing	≤ 2 µs	Pico 2 (HW timer/PWM)	Even energy deposition per pixel
Safety interlocks	Emergency stop, lid switch	≤ 50 µs response	≤ 10 µs	Pico 2 (IRQ + hard cut)	Risk reduction
Watchdog/ fault	Heartbeat loss; disabling laser	≤ 10 ms	N/A	Pico 2 + HW	Failsafe on comms fault

Table 9: Laser Diode Driver Comparison Table

Laser Diode Driver			
Name/Product (Brand)	WLD33ND 3A (Wavelength Electronics)		
Threshold Current (Amps)			

Tony explain laser diode here

3.1.7 Motors

The movement of the laser is of great importance to achieve a fine and precise cut. The movement will be dependent upon the functionality of particular types of motors and motor controllers. The motors to be implemented will move using X and Y coordinates to move the laser accordingly. The type of motor to be used will need to provide the necessary torque to consistently cut in an optimal manner. Most importantly, precision will be best tailored by a motor that can provide small, gradual, calculated movement.

The two main categories of motors are alternating current (AC) motors and direct current (DC) motors. From there, each category has several different kinds of motors. DC motors will best suit this project due to the fact that much of the hardware operates on direct current. It must also be noted that it is simpler to handle control systems with DC motors than with AC motors. Each varied motor will have its advantages and disadvantages. Ultimately, the type of motor to be implemented will have features that most effectively meet the project's needs.

3.1.7.1 Brushed DC Motor

The main parts of this motor include a stator, rotor, brushes and a commutator. The stator produces a static magnetic field around the rotor. The rotor's winding(s) generate a magnetic field when they are supplied with energy. The poles generated from the rotor's magnetic field will come together with the opposite poles from the stator's magnetic field. This coming together of opposing poles will allow the rotor to rotate. When the motor rotates, the brushes will come into contact with many parts of the commutator. A changing magnetic field will be produced inside the motor as a result of a voltage being applied across the brushes. In contrast to brushless DC motors, brushed DC motors do not need a controller to switch the direction of the current. This is due to the fact that it contains brushes and a commutator.

There are some advantages to consider in utilizing a brushed DC motor. For one, the speed of a brushed DC motor is directly correlated to the voltage. Another advantage could be that if only unidirectional rotation is required, and speed and torque do not need to be managed, then no motor controller is needed. Conversely, there are some disadvantages in using a brushed DC motor. For one, the brushes and the commutator are worn out over time. This occurs from the friction when the brushes come into electrical contact with the commutator. For another, the motor is a bit noisy due to the contact between the brushes and the commutator. The noise and brush arcing increases as the motor speed increases. However, it must be noted that the rotational speed is inhibited by the brushes and the commutator. In addition, brushed DC motors have poor acoustic noise and torque ripple.

3.1.7.2 Brushless DC Motor

The main parts of this motor include a stator, a permanent magnet rotor and an electronic controller. This motor is synchronous due to the magnetic field of the stator rotating in equivalent frequency as the magnetic field of the rotor. In contrast to brushed DC motors, brushless DC motors do need a controller to switch the direction of the current. This is due to the fact that it does not contain brushes and a commutator. To attain motor rotation, the stator windings must be supplied with energy in a sequence. The rotor position must be known to know which winding must be supplied with energy. The Hall effect sensors in the stator serve to identify the rotor’s position. From what the Hall sensors identify, the appropriate current is identified to send to the stator to be able to rotate the rotor.

There are some advantages to consider in utilizing a brushless DC motor. This motor does not have the mechanical wear concerns that brushed DC motors have since this motor is brushless. The motor is not noisy thanks to the electronic controller being used for commutation instead of mechanical parts. Unlike brushed DC motors, the rotational speed is not inhibited by brushes. Also, acoustic noise and torque ripple could be decreased by manipulating the winding currents. Conversely, there are some disadvantages in using a brushless DC motor. Due to brushless motors utilizing an electronic controller and possibly using rare earth magnets for the rotor the purchase price is higher than that of a brushed

DC motor. However, it must be noted that the purchase price is higher, but over time it could be money better spent due to the motor experiencing a greater life than brushed DC motors.

3.1.7.3 Servo Motor

The main parts of this motor include the actual motor (DC motor in our case), an encoder or some feedback device, and a controller. The encoder produces signals that specify the angle or displacement of the motor shaft for the purpose of giving feedback on the position of the motor to the controller. The controller uses the feedback signal to change the motor's output, accordingly, in an effort to realize the precise movement. The motor's output is changed by giving it a particular speed, position or torque. An amplifier modifies the voltage or current to adjust the position, torque, or speed accordingly. This use of the feedback signal is what makes it a closed-loop system. The driver circuit drives the motor in a closed-loop system to get to the desired position. The driver adjusts the motor's electrical windings to generate magnetic fields that move the shaft. This motor is built to accurately dictate angular or linear position, velocity and acceleration.

In addition, many servo motors have gears on the shaft to manipulate the motor's output torque and rotation speed. Servo motors have three key operating modes: speed control, torque control and position control. Speed control serves to hold a constant speed despite a change in load. Torque control serves to apply a steady torque in cases where a continuous force is needed. In position control, the motor responds to instructions to move a certain distance or angle.

There are some advantages to consider in utilizing a DC servo motor. For one, a servo motor has a high output power with respect to its size and weight. Another advantage could be that it has a high torque to inertia ratio. Also, the motor can reach a high speed at a high torque. They are not noisy at high speeds. They do not suffer from being out-of-step. Conversely, there are some disadvantages in using a DC servo motor. For one, servo motors need to be tuned to stabilize the closed-loop system. Also, safety circuits are needed in the case of a malfunction. In addition, servo motors are worn out by prolonged overload. Servo motors may also have a higher cost than other motors like stepper motors because of the use of more complex components. Servo motors do not precisely control rotation due to the lag when it is rotating with respect to the command pulses. Most importantly, servo motors vibrate when stopped.

3.1.7.4 Stepper Motor

The main parts of this motor include the stator (has teeth on which coils are wired) and the rotor (which can be a permanent magnet or a variable reluctance iron core). The shaft of the stepper motor rotates by moving a specific number of degrees. The angular position of the shaft is known precisely without the use of a sensor by tracking the number of steps executed. When energy is supplied to one or multiple stator phases, a magnetic field is produced from the current moving in the coil and the rotor positions itself with the field. In energizing various phases in sequence, the rotor is able to rotate by a particular amount to achieve the precise position.

It must be noted that there are three distinct rotor types. For the permanent magnet rotor, it positions itself with the magnetic field from the stator. This allows for an adequate torque and stopping torque. The stopping torque comes from the motor holding itself to a change in position even if a coil has energy. This type of rotor has a lower speed and a lower step size than the other rotors. In the variable reluctance rotor, its shape facilitates its ability to position itself with the magnetic field. This rotor is of an iron core. This rotor is better suited to attain higher speeds and higher step sizes. However, this rotor tends to have lower torque, and it does not have a stopping torque. For the hybrid rotor, it is a combination of the permanent magnet rotor and the variable reluctance rotor. It contains two caps that have alternating teeth, and it becomes magnetic around an axis. A high amount of teeth makes it possible for the motor to attain a short step size of around 0.9°. The stator consists of a certain amount of phases, pairs of poles and wire configuration. The typical stepper motor used is the two-phase stepper motor.

Among the various drivers for stepper motors, the three typical drivers are the Step/Direction driver, the Phase/Enable driver, and the pulse width modulation (PWM) driver. Depending on the driver, it could only regulate the voltage of the winding, or it could additionally regulate the current of the winding. In the case of regulating the voltage, the torque and the speed of how the steps are performed rely on motor and load features. Conversely, torque could be manipulated more effectively in the case that the driver regulates the current of the winding. The direction of the current is also dependent on how the stator coils are structured. The stator coils could be structured in a unipolar manner or in a bipolar manner. A disadvantage of the unipolar stepper motor is the fact that only fifty percent of the copper in the motor is used which results in a magnetic field with half the intensity that would be seen if all of the copper were to be used. Conversely, the bipolar stepper motor is able to maximize torque with respect to how much copper is utilized.

The stepper motor has four distinct driving modes that could be implemented. Wave mode operates by having energy supplied to only one phase at a given moment. For full-step mode, energy is supplied to two phases at a given moment. Full-step mode can achieve a greater torque than wave mode due to a greater current flow and magnetic field coming from the additional phase. Half-step mode is the fusion of wave mode and full-step mode. As hinted by the name, the step size is halved in half-step mode. A disadvantage is that the torque is not stable because it alternates when one phase is supplied with energy and when two phases are supplied with energy. Micro-stepping mode is able to have an even shorter step size while also being able to maintain a constant torque. Micro-stepping mode allows for very precise movement with the tradeoff of low torque for a given step. As the steps are shortened, the resulting torque is lower. This could result in missed steps.

There are some advantages to consider in utilizing a stepper motor. For one, a stepper motor does not need a feedback loop system to know the motor's position. The motor's position is ascertained by counting the number of steps executed. Another advantage is the very precise movement that can be attained with micro stepping. Also, the motor is able to have adequate torque at a low speed. Conversely, there are some disadvantages in using a stepper motor. For one, stepper motors could experience missed steps. This would take away the ability to know the motor's position. Also, the max current is drained even when the motor is stationary which results in overheating and is also a detriment to efficiency. Stepper motors are noisy at high speeds. In addition, stepper motors have a low torque-to-inertia ratio and low power density.

3.1.8 Motor Drivers

Motor drivers are devices that work with a microcontroller to control the operation of motors. Motor drivers provide the necessary voltage, current, protection and direction. From the low voltage signal of a microcontroller, motor drivers are able to provide high power to the motor. This feature is possible due to the motor driver functioning as a current amplifier. Motor drivers can be structured differently, but the most common structure is the H-Bridge. An H-bridge is a circuit that makes it possible to manage the direction of a DC motor. The motor is spun forward or backwards by alternating the polarity of the DC motor. The polarity is dependent on which switches are opened or closed in the H-bridge circuit.

By being connected to a microcontroller, the acceleration and deceleration parameters could be easily modified by the pulse-width modulation (PWM) signal of the microcontroller. This is made possible by the microcontroller sending signals to the motor driver. The motor driver will then decipher those signals, and those signals will be stepped up with the reference voltage to drive the motor. The motor driver will then utilize the two voltage input pins of the motor to manipulate the motor output. One pin will turn ON the motor by providing the reference voltage, and the other pin will turn OFF the motor by providing zero volts at the output. When the microcontroller sends a single HIGH input signal to the motor driver, that is when one input is HIGH while the other input is LOW, the motor driver rotates the motor in one direction. When the input signals are reversed, that is the HIGH input is now a LOW input and vice versa, the motor will rotate in the other direction.

3.1.8.1 A4988 Stepper Motor Driver

When it comes to stepper motors, the A4988 is a commonly used and user-friendly motor driver integrated circuit (IC). It is compact with dimensions of 0.6 in. x 0.8 in. and a weight of 1.3 g. It has two board layers, and it is a low-cost stepper motor driver. The driver operates from a minimum operating voltage of 8 V to a maximum operating voltage of 35 V. It can provide a maximum continuous current per phase of 1 A, and it can provide a peak current per phase of 2 A. These ratings make it suitable for small to medium-sized stepper motors. The driver offers micro-stepping from a full step, 1/2 step, 1/4 of a step, 1/8 of a step, and 1/16 of a step. This means that a full step can be broken all the way down to 16 smaller, equivalent micro-steps.

The A4988 contains a built-in translator that makes it easier to control stepper motors. With the translator, only two pins need to be controlled. One pin commands the motor to move a step, and the other pin commands the motor to move in a particular direction. The driver offers many safety features which include short circuit protection, under-voltage protection, thermal shutdown, shoot-through protection, and overcurrent protection. The driver provides 16 total pins. The VDD and GND pins provide power to the internal logic circuitry, The VMOT pin and a different GND pin provide power to the actual stepper motor. The MS1, MS2 and MS3 pins can be set to several HIGH or LOW combinations to achieve one of the five micro-stepping modes. If all of the pins remain disconnected, then the motor will be in full step mode. The STEP and DIR pins are for control. STEP is for the motor to perform steps. DIR dictates the direction of the motor. The EN, RST and SLP pins are for power control. The EN pin enables or disables the driver. The SLP pin places the A4988 into a power-saving sleep mode. The RST pin resets the A4988 when pulled LOW. The 1A, 1B, 2A and 2B pins are for the motor's output. These pins connect the driver to the stepper motor.

Although the A4988 has a maximum current rating of 2 A, the typical current that can be delivered relies on maintaining the chip cool. Absent of any cooling, the driver can operate around 1 A before it overheats. To operate safely above 1 A, a heatsink or other cooling medium must be used. Stepper motor performance can be enhanced by providing the stepper motor a higher voltage than what it is rated for. Being able to safely operate the motor with a higher voltage than what it is rated for is made possible by limiting the current flowing through the coils of the motor. This can be done by manipulating the current limiting potentiometer on the A4988.

3.1.8.2 TMC2209 Stepper Motor Driver

The TMC2209 is a very silent stepper motor driver built for two phase stepper motors. The driver operates from a minimum operating voltage of 4.75 V to a maximum operating voltage of 29 V. It can provide a maximum continuous current of 2 A RMS, and it can provide a peak current of 2.8 A. The driver contains pins that offer micro-stepping from 1/8 of a step, 1/16 of a step, 1/32 of a step, and 1/64 of a step. Beyond the micro-stepping offered by the pins, micro-stepping from full step all the way down to 1/256 of a step is possible by implementing the MicroPlyer™ interpolation feature using the UART interface. The StealthChop2™ feature allows for complete silence of the motor when in operation and when it is idle. The StallGuard4™ feature can warn of motor overload. The CoolStep™ feature allows for current control to save energy up to 75%. The driver offers many safety features which include overcurrent protection, undervoltage detection, thermal shutdown, short circuit protection, and under-voltage detection.

3.1.8.3 TB67S581FNG Stepper Motor Driver

The TB67S581FNG is a two-phase bipolar stepper motor driver IC manufactured by Toshiba. The driver has dimensions of 0.6 in. x 0.8 in. and has a weight of 1.6 g. It comes with four board layers, and it is a low-cost stepper motor driver. The driver operates from a minimum operating voltage of 8.2 V to a maximum operating voltage of 44 V. It can provide a maximum continuous current per phase of 1.5 A, and it can provide a peak current per phase of 2.2 A. The ability to operate under the continuous current of 1.5 A is when a heatsink or some other cooling medium is not used. However, if the necessary cooling medium is implemented then the TB67S581FNG can operate up to the peak current of 2.2 A. The driver offers micro-stepping from a full step, 1/2 step, 1/4 of a step, 1/8 of a step, 1/16 of a step, and 1/32 of a step.

The driver offers many safety features which include under voltage lockout detection, thermal shutdown detection, short-to-ground and shorted-load protection, and overcurrent detection. Several decay modes are provided such as mixed decay, slow decay and fast decay. It also includes a sleep mode which serves to save power. Higher step rates can be achieved by providing the stepper motor with a higher voltage than what it is rated for. This is made possible by limiting the current flowing through the coils of the motor. This can be done by manipulating the current limiting potentiometer on the TB67S581FNG.

3.1.8.4 DRV8825 Stepper Motor Driver

The DRV8825 is a commonly used and user-friendly motor driver integrated circuit (IC) manufactured by Texas Instruments. It has four board layers, and a compact size of 0.6 in. x 0.8 in. and a weight of 1.6 g. The DRV8825 is the most expensive when compared to all of the aforementioned stepper motor drivers but it is still affordable. The driver operates from a minimum operating voltage of 8.2 V to a maximum operating voltage of 45 V. It can provide a maximum continuous current per phase of 1.5 A, and it can provide a peak current per phase of 2.2 A. Being able to operate under the continuous current of 1.5 A is when a heatsink or some other cooling medium is not used. However, if the necessary cooling medium is implemented then the DRV8825 can operate up to the peak current of 2.2 A. The driver offers micro-stepping from a full step, 1/2 step, 1/4 of a step, 1/8 of a step, 1/16 of a step, and 1/32 of a step. This means that a full step can be broken all the way down to 32 smaller, equivalent micro-steps.

The DRV8825 utilizes a simple step and direction interface which works by the motor executing a step and moving the motor in a particular direction, respectfully. The driver offers many safety features which include short-to-ground and shorted-load protection, under-voltage lockout, over-temperature thermal shutdown, and overcurrent shutdown. Higher step rates can be reached by providing the stepper motor with a higher voltage than what it is rated for. This is made possible by limiting the current flowing through the coils of the motor. This can be done by manipulating the current limiting trimmer potentiometer on the DRV8825.

The driver contains 16 total pins. The VMOT and GND pins provide power to the driver itself and the actual stepper motor. The M0, M1 and M2 pins can be set to several HIGH or LOW combinations to achieve one of the six micro-stepping modes. If all of the pins remain disconnected, then the motor will be in full step mode. The STEP and DIR pins are for control. STEP is for the motor to perform steps while DIR dictates the direction of the motor. The EN, RST and SLP pins are for power control. The EN pin enables or disables the driver. The SLP pin places the DRV8825 into a power-saving sleep mode. The RST pin resets the DRV8825 when pulled LOW. The FAULT output pin goes LOW after the DRV8825 is triggered by one of the many safety features. When this pin is activated, the driver is disabled for protection. The driver is able to return to normal upon activating the RST pin or by disconnecting and reconnecting the VMOT pin. The A1, A2, B1 and B2 pins are for the motor's output. These pins connect the driver to the stepper motor. The A1 and A2 pins connect to one coil while the B1 and B2 pins connect to another coil.

3.2 Software Research

3.2.1 Operating System and Language

Table 10: Operating System and Language Table

Layer	**Option**	**Pros**	**Cons**	**Fit for Project**
OS	Raspberry Pi OS	First-party support for Touch Display 2 Easy Kiosk setup	Not hard real time Potential jitter under load when it comes to timing	Chosen, best balance for UI support and stability
	Ubuntu	Long term stability and security support Support snap containers	More resource intensive Slower boot Requires manual configuration	Not needed for what its offering compared to the Raspberry Pi OS that offers better integration

			for the touch display	
Language	Python	Faster Iteration and good critical timing Simple/Large Library Support	Slower as python is interpreted and not compiled	Chosen, ideal for UI logic and serial communication to MCU
	C/C++	Compiled language with timing that is more predictable Minimal memory use; efficient for embedded environments	More complex syntax and manual memory management Prone to low level bugs	May be used on microcontroller side for real time PWM, interlocks, and safety control

Our project uses a Raspberry Pi 4B running Raspberry Pi OS (a Linux-based system) as the primary operating system, chosen for its strong community support, open-source libraries, and great compatibility with embedded peripherals; especially with our chosen touchscreen. The Pi will operate in kiosk mode, ensuring that the only visible and running application is our system's graphical interface. This approach simplifies operation and reduces the chance of user error, and implementation is straightforward thanks to official Raspberry documentation serving as a guide.

However, the project also demands precise timing and deterministic control, which are difficult to guarantee when the HMI runs on a general-purpose multitasking OS like Linux. Since Linux schedules tasks dynamically (meaning the operating system continuously decides which process gets CPU time based on priority, load, and background activity), timing can vary slightly from one event to another. These small variations, or Jitters, are negligible for normal operations like updating the screen or reading user input, but they might become a problem when trying to use precise control signals when it comes to laser control and safety concerns. Even with PREEMPT_RT real-time patch, which improves kernel preemption and significantly lowers average scheduling latency, the system remains "soft real-time" rather than "hard real-time." Researchers at the Max Planck institute for Software Systems measured latencies under load reaching several hundred microseconds to a few milliseconds in PREEMPT-RT Linux[20]. Such jitter is unacceptable for microsecond-sensitive operations like laser PWM gating or safety interlocks, which require strict and repeatable response times.

To resolve this, real-time control will be delegated to a dedicated microcontroller running compiled C/C++ firmware. This division allows the Raspberry Pi to handle high-level tasks such as the user interface, job management, and file transfers, while the microcontroller executes timing-critical operations with deterministic precision. This hybrid structure combines the Pi's flexibility with the microcontroller's reliability, ensuring both a robust HMI with a safe and accurate laser control.

3.3 Optical Design

3.3.0 Laser Source Considerations

When comparing laser sources, we considered fiber, CO2, solid-state, and semiconductor lasers. These were the main types used in different types of laser cutting, including cutting metal and non-metal objects. These of course are within the visible wavelength spectrum since an infrared wavelength would be hard to align without an infrared viewing card. The most common type of laser used for non-metallic objects are CO2 lasers, while fiber lasers will work with most materials although they are limited in the material thickness they can cut.

The basics components of a laser are the gain medium, pump mechanism, optical resonator or cavity, and the output coupler. The pump mechanism supplies energy to the gain medium, inciting a population inversion and causing stimulated emission of photons. This emission of photons is reflected by the optical cavity mirrors and passes through the gain medium inside, causing amplification before exiting through the output coupler shown as R2. This output coupler can be a partially transparent mirror or a pulsed shutter that allows for a fraction of the beam to exit the cavity[13].

CO2 lasers are gas-discharge lasers that use electricity to vibrate CO2, or carbon dioxide, molecules. This involves inducing an electric field over a gas tube full of a specific ratio of N2 to CO2 gas with hydrogen, xenon, and helium. The ends of the laser tube have Brewster mirrors, one half silver and the other fully silver. With powers ranging from watts to kilowatts and a wavelength of either 10.6 or 9.6 micrometers, this laser type can be very useful for industry applications when cutting materials more than 20 millimeters thick[12]. We chose to forgo pursuing this option because it would be difficult for us to ensure the correct gas ratios in the gas chamber/tube when building this laser.

Fiber lasers use a doped fiber optic strand as the gain medium, coupled between the laser cavity mirrors to create stimulated emission of photons. The wavelength emitting from these lasers is dependent on the doping of the fiber. For example, ytterbium doped fibers emit a wavelength of around 1060 nanometers, and these are a typical doping choice for the fiber. These are compact and low maintenance and are commonly used for laser cutting metals because their wavelength is more effective than other types of lasers. The main reason for not pursuing this type of laser was inexperience with fiber lasers and the possibility of too much power incident on the fabric while cutting.

The laser that most people imagine are typically the Nd:YaG lasers that use an Nd:YaG crystal as the gain medium. This is a solid-state laser due to its use of a crystal as the gain medium. The wavelength of a solid-state laser is dependent on the crystal used, and the wavelength from Nd:YaG is 1064 nanometers. An Nd:YaG laser is suitable for laser cutting of both metals and non-metals but requires active cooling and potential maintenance of the crystal.

Laser diodes are semiconductor lasers due to the use of a semiconductor PN junction as the gain medium. Our specific laser diode uses InAlGaN as the chip, giving us the low wavelength of 445-465 nanometers and laser diodes can produce wavelengths from 375 to 2000 nanometers depending on the chosen semiconductor. The resonator cavity needed to pump the laser is already built into our diode, negating the need for a pair of mirrors to form the optical cavity around the laser like those needed in CO2 lasers.

Considerations were given into the power needed to cut through different types of fabrics. However studies revolving these topics focus on the power of the laser, not the actual incident power from the beam. Because of this it is not valid to correlate wattage of lasers to actual power going into the material, in our case fabric. This is why the previous senior design group was able to use a 3-5 watt laser to safely engrave paper without cutting completely through it. With any laser cutting project, there must be significant consideration into the cutting speed to ensure there is not a high-powered laser resting on the cutting material for too long, potentially igniting the material. Because of this concern, we knew a laser diode would be our best option as it has the lowest power when compared to the other types of lasers.

3.3.1 Laser Diode Comparison Table & Description

Table 11: Laser Diode Comparison Table

Laser Diode			
Name/Product (Brand)	455nm 5500mW Laser Diode	455nm 3500mW Laser Diode	405nm 3.3W Laser Diode

	(LaserTree)	(LaserTree)	(LaserTree)
Threshold Current (Amps)	.24-.44	.25-.33	.43-.53
Operating Current (Amps)	3.5	2.1-2.4	1.6-2.2
Operating Voltage (Volts)	3.5-4.7	4.4-5.2	4.7-5.5
Typical Wavelength and Range (Nanometers)	455 445-465	455 445-465	405 400-415
Output Power (Watts)	5.5	3.5	3.3
Cost (USD)	55	25	285

For F.L.C.S we decided to go with a laser diode system because of its compact size and due to our inexperience with CO2 lasers, a common method for cutting textiles. Using laser diode for our beam source allows us to adjust the power of the laser for varying fabric thicknesses, due to the linear relationship between threshold current and output power or light [13]. Prior to hitting the threshold current, the laser diode operates like an LED, yet afterwards it operates as a laser with increasing output light as current increases. A previous senior design project at our university successfully designed an engraving system using a 405 nm, 500 milliwatt laser diode [5].

When choosing the specific laser diode for our system the first concern was the amount of power and absorbance of wavelengths that allow for burning through fabric. El Sherif provides information regarding the typical absorption found in polyester between wavelengths 400 and 460 nm, we know that the absorption will be higher around 400 nm than 450 nm. However when accounting for varying red, yellow, and blue dye concentrations, 450 nm is a wavelength that will have more uniform absorption across different colors [14]. Because of this in tandem with the previous senior design groups' performance, I believe we should be able to cut through fabrics with our 455 nm 3W laser diode. The graph to the right represents a pseudo-absorption diagram using measured reflectance, R [15]. As you can see on the right, throughout the visible spectrum, 380-750 nm, wavelengths less than 500nm are absorbed better into textiles or fabric, allowing the fabric to burn easier and with less power or passes needed by the laser. With our financial constraints, we were unable to find 400 nm laser diodes with the minimum of 3 watts needed to burn through the fabric.

3.3.2 Lens Comparison Tables & Descriptions

Table 12: Aspheric Lens Comparison Table

Beam Shaping Optics			
Name/Product (Brand)	**C710TMD-A Aspheric Lens (Thorlabs)**	**C140TMD-A Aspheric Lens (Thorlabs)**	**PS873-A Anamorphic Prism Pair (Thorlabs)**
Focal Length (mm)	1.5	1.5	N/A
Design Wavelength (nm)	1550	780	405
Cost (USD)	111.17	104.03	203

To start our lens system, we will first correct our elliptical beam shape from our laser diode into a circular beam. This can be done in a few different ways. A baseline to help shape the beam is by using circular cylinder lenses throughout our system, but we must first collect the beam from the laser diode and use either an aspheric lens or anamorphic prism pair to force the beam shape. If a circular cylinder lens was used directly after the laser diode, the excess light in the vertical direction could pass over the edge of the lens, introducing stray beams into our enclosure. We focus on expanding the beam because expanding the beam prior to focusing ensures we will have a small spot size incident on the fabric [16].

Using an anamorphic prism pair as our main beam shaping optic allows us to correct the aspect ratio of the beam, as opposed to using multiple spherical lenses that would shape the beam but would change the polarization. Because the anamorphic prism pair is unmounted due to financial constraints, we will be utilizing 3D printing to mount the lens in the required position to effectively reshape the beam. Since light diverges as it travels, we prioritized having a shorter lens system to minimize divergence and to best suit the size of our enclosure. Although our chosen aspheric lens has a design wavelength of 780 nm, this will not have an impact on the lens system due the focal length varying slightly for different wavelengths. Because of this we will be adjusting the distance between this lens and other optical components prior to our demo to ensure the distance is correct even if the focal length is slightly different.

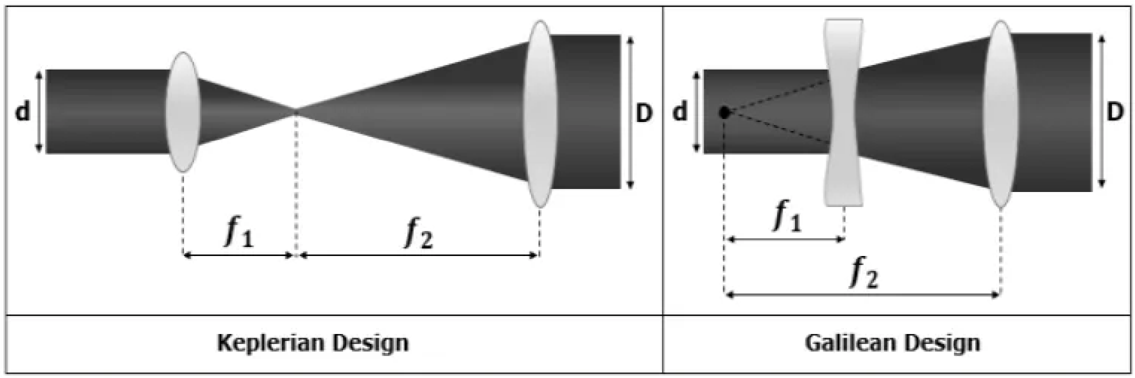

Figure 10: Keplerian and Galilean Lens Systems [17]

For beam expansion there are a couple of systems we can utilize to best expand the beam before it reaches the focusing lens. These systems are called Keplerian and Galilean. For our system we choose to utilize a Galilean beam expander because it does not focus the light into a singular spot, like the Keplerian system shown in Figure 11 above. Using a Keplerian system would create a hot spot in our system prior to contact with the fabric. Additionally, using a Galilean system enables us to have a smaller length lens system than the Keplerian counterpart. Expanding our beam prior to contact with the focusing lens decreases divergence and ensures a smaller spot size incident on the fabric [12].

Table 13: Beam Expander Lenses Comparison Table

Lenses for Beam Expander			
Plano-Concave Lenses			
Name/Product (Brand)	**LA6002 (Thorlabs)**	**LA8126-E (Thorlabs)**	**LC1975 (Thorlabs)**
Back Focal Length (mm)	45	19.3	-25.4
Reflective Coating Range (nm)	N/A	1000-6000	N/A
Design Wavelength (nm)	465	4000	587.6
Material	Magnesium Fluoride	Silicon	NBK-7
Diameter (mm)	25.4	12.7	6
Cost (USD)	387.66	286	28.72
Convex Lenses			

Name/Product (Brand)	Bi-Convex Lens LB1945-AB (Thorlabs)	Plano-Convex LA1613 (Thorlabs)	Bi-Convex Lens LB4265-A (Thorlabs)
Back Focal Length (mm)	198.4	125	149.4
Diameter (mm)	25.4	12.7	25.4
Cost (USD)	45	28.7	132.68

When designing the beam expander expansion system we focus on plano-concave and plano-convex lenses because combining these will help us expand our beam. The laser diode beam will diverge, or spread, after the plano-concave lens and converge after the convex lens. Utilizing a biconvex at the end of this lens system enables the beam's size to be almost constant as the distance from the lens increases, making it a nearly collimated beam when placed at the correct distance from the plano-concave lens. Whereas when using a plano-convex lens, like we originally accounted for, the beam can expand until it reaches the maximum allowed by the size of the previous lens.

We focused our attention on the back focal length of these lenses due to its involvement in the magnification formula of a Galilean beam expander. Having a large back focal length would result in less beam expansion, and using a pair of lenses with positive back focal lengths would ensure our system magnifies the beam instead of expanding it.

Most of our lenses have an anti-reflectance (AR) coating that minimizes loss. An increase in loss corresponds to lower power incident on the fabric. We avoided lenses such as the LA3803-E due to their reflectance coating being in the range of 2-6 micrometers, which would not minimize loss for our diode's typical wavelength of 455 nanometers. The AR coating covering the aspheric lens and anamorphic prism pair works for wavelengths 350-700 nm, whereas the bi-convex has a range of 400-1100 nm. Additionally, we prioritized looking at cheaper lenses, mainly those made of NBK-7, a common glass type that doesn't fracture easily and is relatively easy to manufacture. The only concern with NBK-7 is the heat tolerance but with our low laser power and short run times we do not need to be concerned.

3.3.3 Mirrors Comparison Tables & Descriptions

Table 14: Mirrors Comparison Table

Mirrors			
Specifications	**Fused Silica Broadband Dielectric (E02)**	**Protected Silver**	**Protected Aluminum**

Reflectivity (455 nm)	>99%	>97%	>90%
Bandwidth	Moderately broad 400nm - 750nm	Very broad 450 nm - 2 µm	Very broad 450 nm - 2 µm
Absorption	<1%	<3%	<10%
Laser Damage Threshold	High threshold (470 W/cm)	Moderate threshold (213 W/cm)	Low threshold, lot of power absorbed (43 W/cm)
Surface Quality	High quality, laser-grade, low scatter (10-5 Scratch-Dig)	Good quality, good for optics (40-20 Scratch-Dig)	Good quality, good for optics (40-20 Scratch-Dig)
Cost	Most expensive $50-$60	Least expensive ~$30	Moderately expensive ~$40

When considering how to best direct the laser beam onto the fabric, some different properties of the mirrors were taken into account such as reflectivity and overall quality. Based on the different options from the table, it seems like using dielectric mirrors would work the best for this system. Compared to the other materials, it is the highest quality and absorbs the least amount of light from the beam. The only downside to having dielectric mirrors over a moderately good mirror like protected silver is that it is a more expensive option.

For dielectric mirrors, they are available with different coatings which reflect best at different ranges of wavelengths, shown on the graph below (Thorlabs). Using the information displayed, it can be determined that both E01 and E02 coatings could work sufficiently for the beam wavelength being used, but E02 has slightly more reflectance over E01.

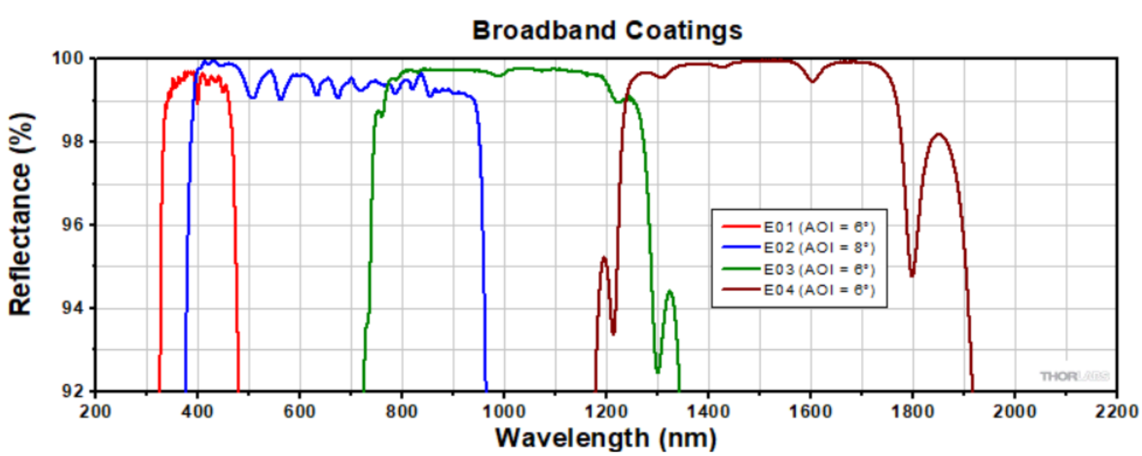

Figure 10: Reflectance of dielectric mirrors with each of the different coatings available from E01 to E04 on Thorlabs. [21]

3.3.4 Focusing Lens Comparison Tables & Descriptions

After the mirrors, a focusing lens is used to increase the on-sample peak irradiance. Because some fabrics are thick or may require multiple passes, a longer focal length is often preferred to provide sufficient working distance between the lens and the fabric.

3.3.4.1 Spheric and Aspheric Lens Comparison

Common economical lens types are plano-convex, bi-convex and aspheric lenses. Plano-convex and bi-convex lenses are widely available in many sizes and focal lengths, but spherical lenses introduce spherical aberration that enlarges the focused spot and reduces the achievable peak intensity. Aspheric lenses correct much of the spherical aberration and can produce a smaller, closer-to-diffraction-limited spot, but they are typically more expensive.

To simulate the magnitude of the spherical aberration produced by spherical lenses compared to aspheric lenses, Zemax can be used to show the final spot size aberrations at the focal point of each type of lens at 455nm wavelength. They all also show the airy disk, the smallest spot size attainable due to diffraction. Ideally, the aberrated spot size should be close to or smaller than the airy disk.

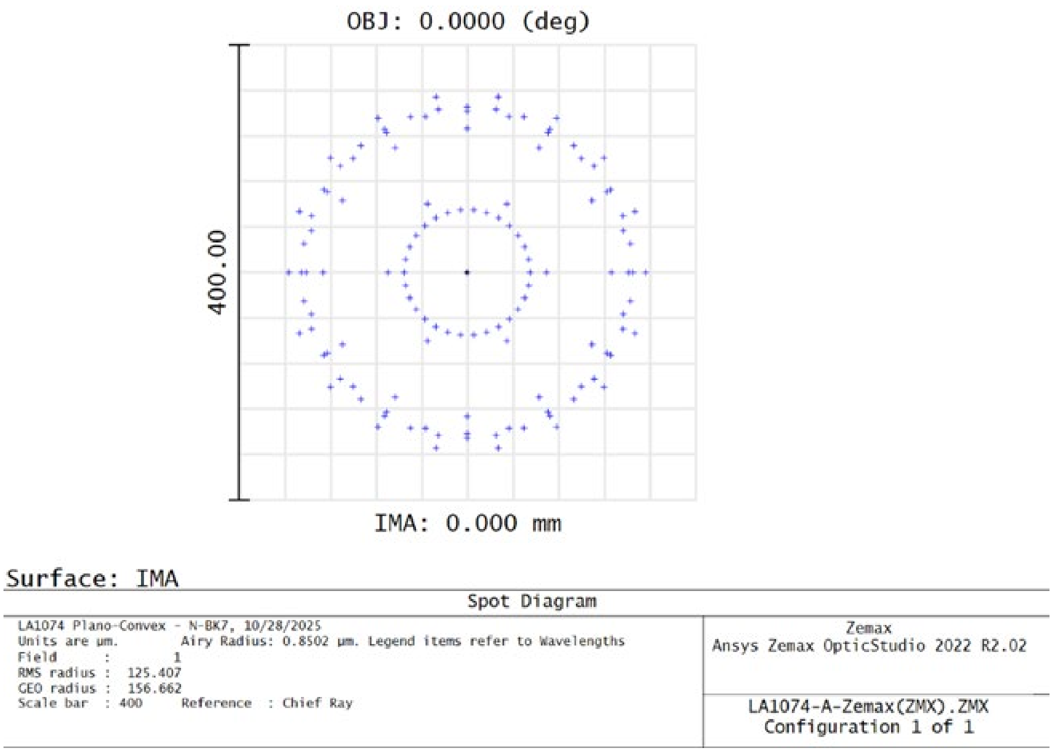

Figure 11: (LA1074-A) Plano-convex 19.6 mm focal length lens, minimum spot size 313.324 µm (Zemax)

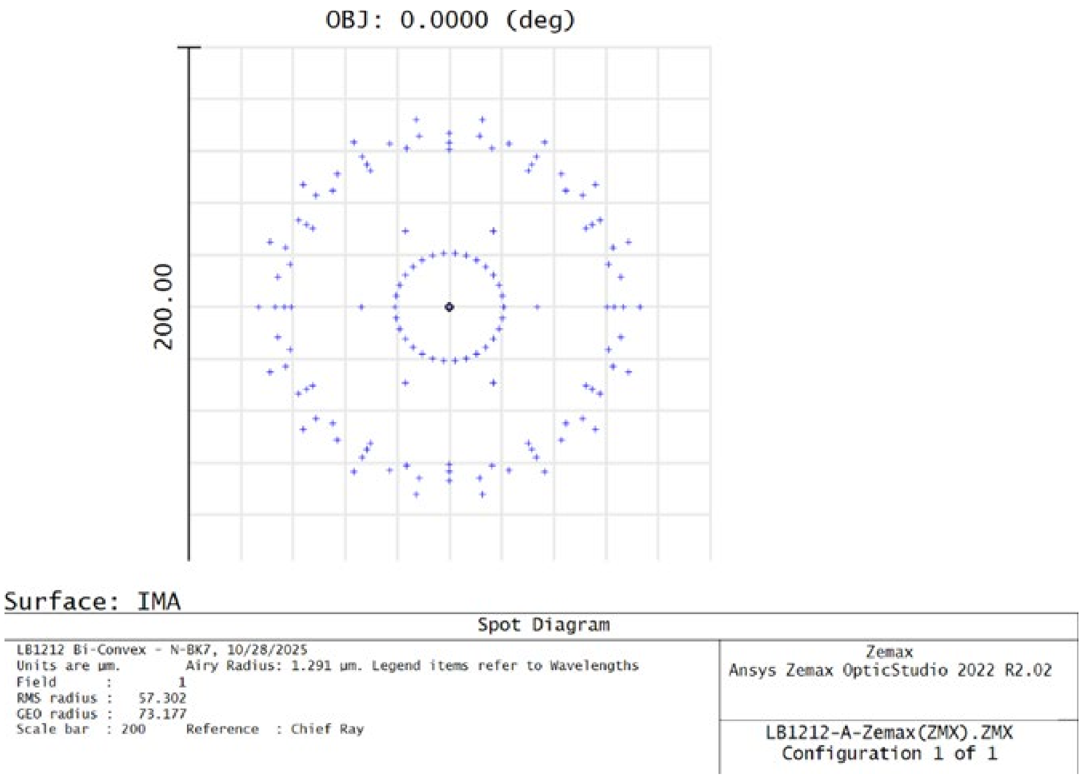

Figure 12: (LB1212-A) Bi-convex 19.6 mm focal length lens, minimum spot size 146.354 µm (Zemax)

In both figures, the airy disk is so small that it is barely visible or not visible at all. Compare the size of the airy disk and the overall aberrated size of the spot produced by the aspheric lens to the above spheric lenses.

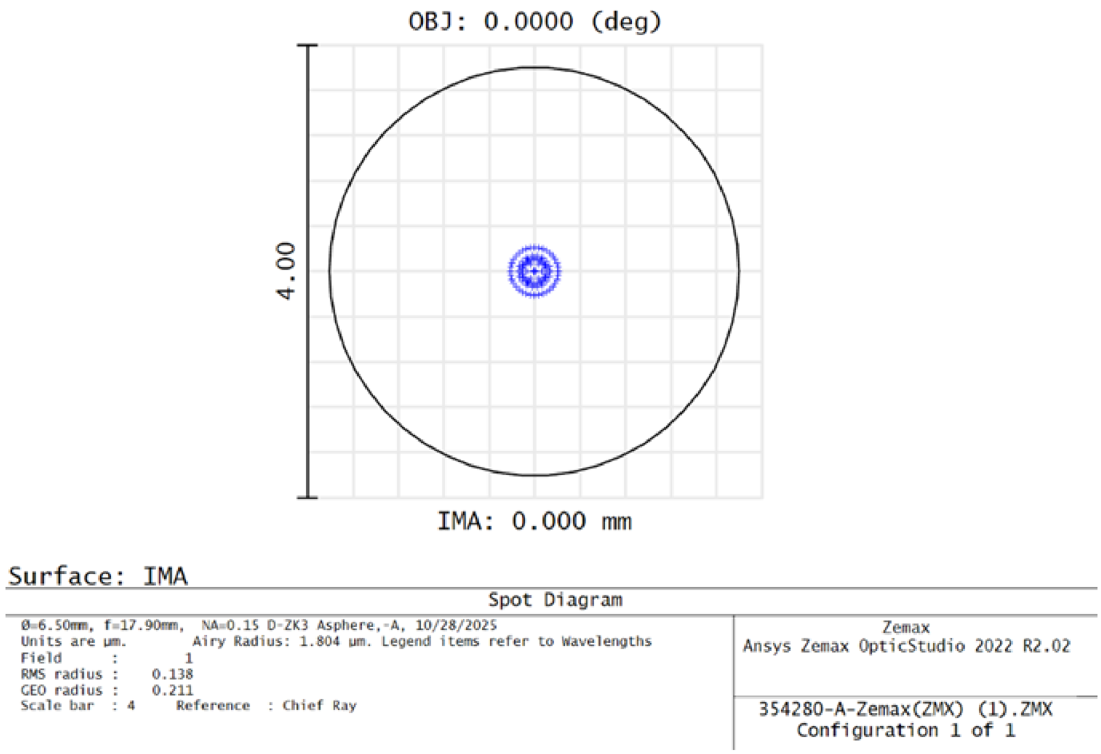

Figure 13: 354280-A: Aspherical 17.9 mm focal length lens, minimum spot diameter of 0.422 µm. Due to diffraction, the actual spot diameter is 3.608 µm. (Zemax)

As can be seen in the figures above, the aspherical lens is far superior to the plano and bi convex lenses when it comes to focusing the laser to a small spot, with the smallest spot size achieved by the aspherical lens being three magnitudes smaller than the other lenses.

3.3.4.2 Deciding an Aspheric Lens

When searching for aspheric lenses, as much optical power should traverse through the lens as possible, so an aspheric lens with an AR coating would be desirable.

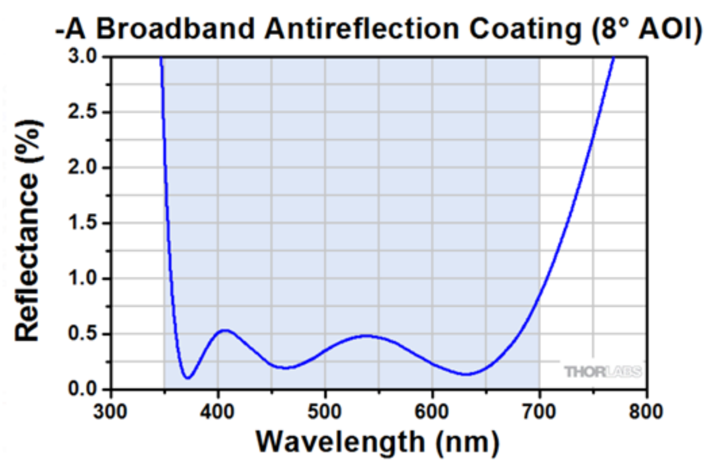

Figure 14: Graph of the AR coating's reflectivity against the incident wavelength. The coating appears to have a reflectance of about 0.25% at 455 nm. [22]

The effective focal length is only accurate for a specific wavelength, noted as the "design wavelength". Most of the wavelengths the specifications are designed around are between 600 nm to 800 nm. Due to chromatic dispersion, those specifications listed would not be accurate, since the focal length would be a shorter distance for 455 nm. For example, the lens 354280-A was designed at 780 nm and had a recorded effective focal length of 18.4 mm. When 455 nm was sent through the lens instead, the actual effective focal length of the lens shortened to 17.9 mm. [22]

Aspheric Focusing Lens		
Specifications	A280-A https://www.thorlabs.com/thorproduct.cfm?partnumber=A280-A	354280-A https://www.thorlabs.com/thorproduct.cfm?partnumber=354280-A
Effective Focal Length (455 nm)	17.8 mm, slightly shorter	17.9 mm, farthest
Coating	AR (350 nm – 700 nm)	AR (350 nm – 700 nm)
Spot Diameter at Focal Point (455 nm)	11.256 µm aberrated spot size, not diffraction limited by airy disk, good quality	0.422 µm aberrated spot size, diffraction limited by airy disk with 3.608 µm diameter, best quality
Lens Diameter	6.5 mm	6.5 mm
Cost	$98.83	$83.90

Table 15: Focusing Lens Comparison Table

From Thorlabs, there were really only two unmounted aspherical lenses which seemed like appropriate options, especially since these lenses had the longest effective focal length out of any of the other aspheric lenses available on the website.

3.3.4.3 Focusing Lens Calculations

In the setup for the laser system being used, the collimated input beam diameter is significantly smaller than the focusing lens aperture. In this case, using the Gaussian equations for calculating the intensity of the final spot would be the most accurate. To find the peak on-axis intensity of the spot, the spot radius at the waist with intensity at least $\frac{1}{e^2}$ of the maximum (ω_0) must be found along with the oncoming power of the collimated beam onto the lens.

$$\omega_0 = \frac{f\lambda}{\pi\omega_i}$$

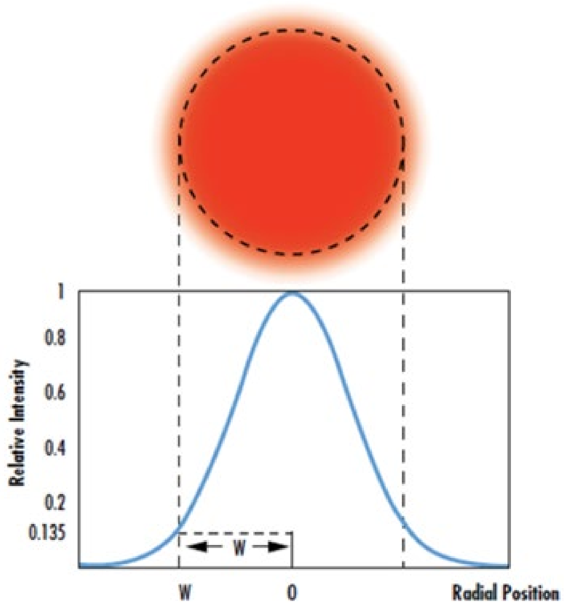

Figure 15: Visualization of the radius (W) of the waist which has $\frac{1}{e^2}$ of the maximum intensity. [27]

The desired wavelength of the light is 455 nm (λ) and the focal length at this wavelength is 17.9 mm (f). At this moment, the exact expected beam radius incident onto the lens is not certain, only that it is significantly smaller than the lens radius (3.25mm), so for simplicity it will be assumed that the incident beam radius is 1mm (ω_i). With these parameters, the spot radius at the waist is calculated to be 2.59 µm. Though, if the incident beam radius which could be achieved could be expanded into an area with an even larger radius, then the focused spot size could be reduced even further.

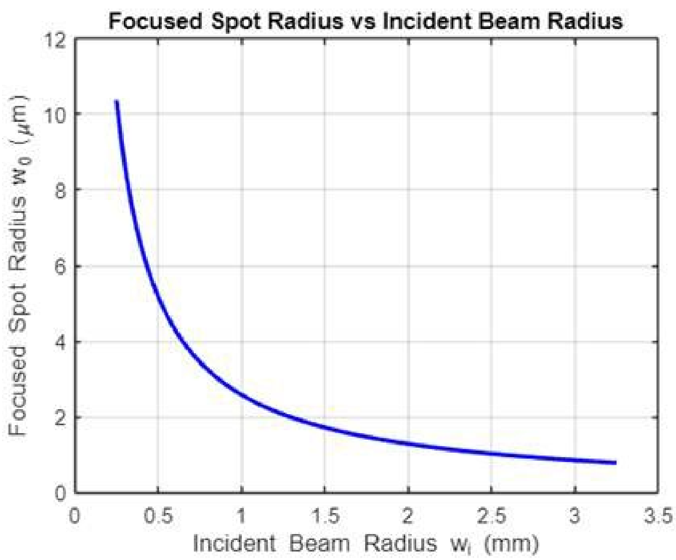

Figure 16: Graph illustrates the relationship between the incident beam size and the final spot size. (MATLAB)

The output power (P) of the laser system will be roughly 3W. This amount of power is extremely high for a laser beam and will result in a very high intensity spot for cutting.

$$I_0 = \frac{2P}{\pi {\omega_0}^2}$$

Since, again, the oncoming collimated beam will have an assumed radius of 1 mm, the peak intensity of the spot with these parameters is $2.84 * 10^5\ W/mm^2$. If the spot size into the lens could be increased, the intensity onto the fabric could increase significantly, as can be seen in the graph below.

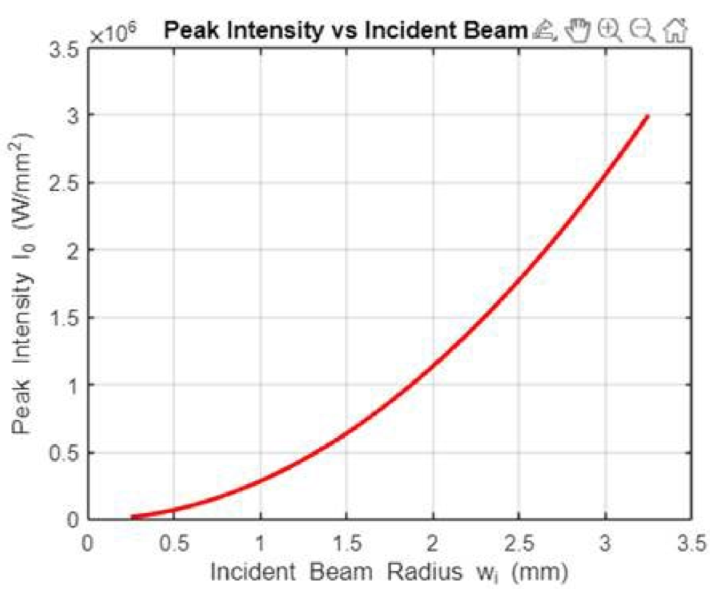

Figure 17: Relationship between the incident beam size and the spot peak intensity. (MATLAB)

Using the peak intensity of the spot, the Gaussian intensity profile of the final spot can be graphed to accurately predict what the spot will look like incident onto the fabric, given that it is smooth and flat on the canvas with minimal wrinkles.

$$I(r) = I_0 e^{-2(\frac{r}{\omega_0})^2}$$

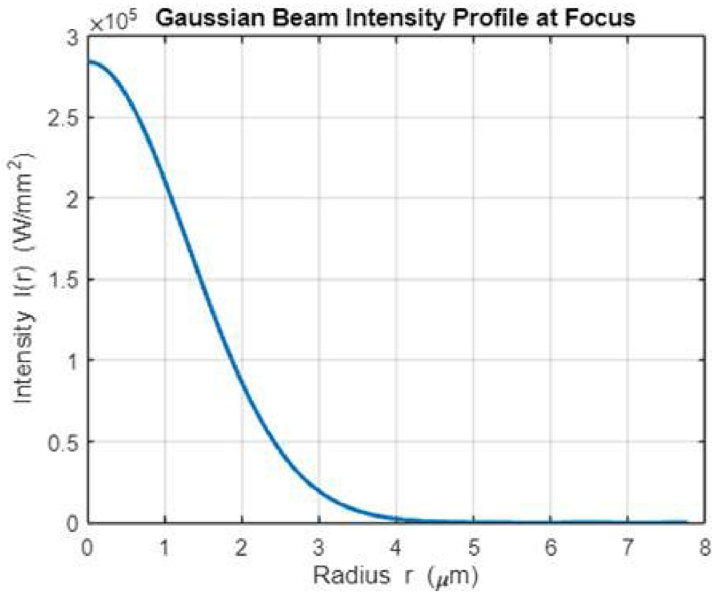

Figure 18: Focus spot intensity profile at input radius at 1mm (MATLAB)

This intensity profile is only attainable if the distance between the focusing lens and the fabric are at a very specific distance from each other due to the small Rayleigh range of the focus spot. The Rayleigh range is the distance from the beam waist where the spot radius increases by a factor of square root 2.

$$z_R = \frac{\pi {\omega_0}^2}{\lambda}$$

Using the equation above to find the Rayleigh range, it is $46.4\ \mu m$, which is incredibly small. This means, depending on the roughness of the fabric and the smoothness of the overall operation of the gantry system, that the likelihood of the spot on the fabric is not very likely to be within the Rayleigh range most of the time.

$$\omega(z) = \omega_0 \sqrt{1 + \left(\frac{z}{z_R}\right)^2}$$

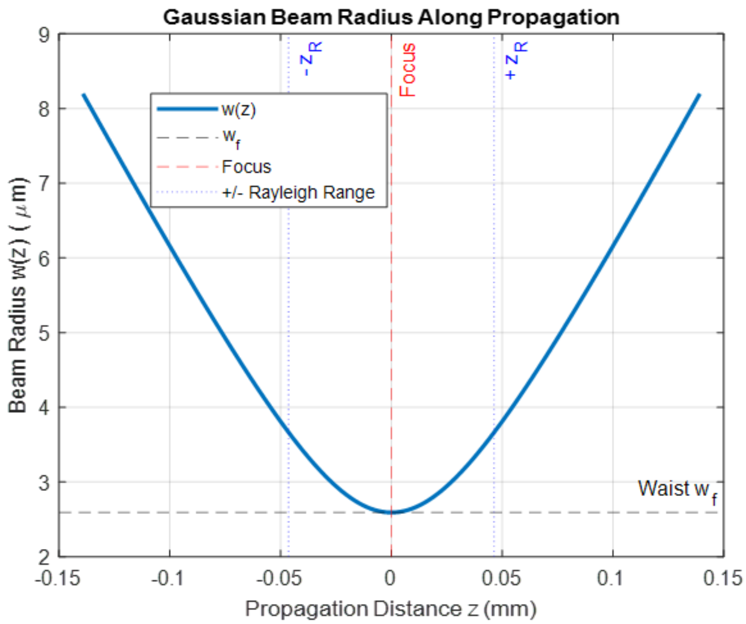

Figure 19: The Gaussian beam propagated near the focal point of the focusing lens (ω_i = 1 mm). The positive and negative Rayleigh ranges are labeled $-z_R$ and $+z_R$. The range between $-z_R$ and $+z_R$ is the depth of focus. (MATLAB)

Using the above equation, the Gaussian beam radius of the spot can be visualized with respect to the distance from the focusing distance. If the radius of the beam into the lens expands larger than the default 1mm, the Rayleigh range would be even smaller and hence the likelihood of the spot being within the Rayleigh range becomes even smaller.

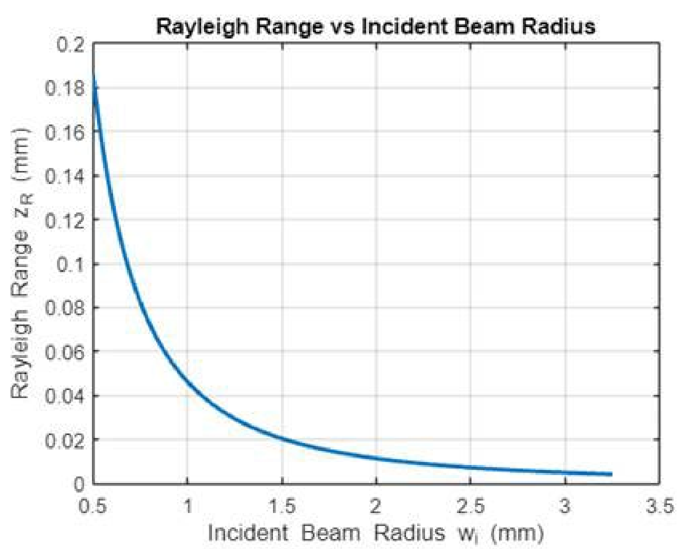

Figure 20:The relationship between the incident beam radius and the Rayleigh range. (MATLAB)

3.3.4.4 Effects of Spot Characteristics and Cutting Speed

The final spot size plays a critical role in how clean and efficient the cut will be. Although articles on laser cutting fabrics are scarce, much more is known about cutting other materials. Though they are not fabric, many of the same characteristics can be applied to them.

When the spot size is small, the intensity is maximized, meaning finer details can be cut more quickly. Since the beam energy is concentrated into a smaller area, the required exposure time in an area to cut through the material is decreased. In this case, the gantry head can move faster and finish a cut quicker. However, as the spot size decreases, the depth of focus shrinks. For thick or uneven fabrics, a shallow depth of focus can degrade cut quality. If the surface of the fabric is outside of the depth of focus, the beam area expands, intensity drops, and the cut may not penetrate cleanly. [28, 29]

Alternatively, if the spot size is too large, then the intensity of the spot is much lower, meaning more time is required to achieve the same cut depth. A larger spot tends to reduce precision, increases the cut width, and can lead to rougher, less defined edges. The material removal is less efficient because the energy is spread over a larger area. The sensitivity to focus and fabric height variation is reduced, but at the cost of cut quality and speed. [30]

If the power is being adjusted instead of spot size, the effect on the final spot intensity of the power being excessively high is equivalent to the spot size being excessively small, and vice versa.

Intensity may need to be adjusted when changing the fabric material, changing the final size of the shape, or when the material surface is uneven. For instance, a thicker fabric may cut more effectively with a larger spot size and higher power so that the beam remains effective across variations in height and ensures it is cut all the way through, given the case it is set to be cut in a single pass. Meanwhile a delicate fabric may necessitate reducing power to avoid unwanted damage.

To adjust the final spot on the fabric, both the spot size and the source laser power are valid for adjustment, but they both have trade-offs. Adjusting laser power, with constant spot size, increases intensity directly and can speed up processing or enable thicker cut-through, but it also increases thermal load and risk of damage. Adjusting spot size, with laser power held constant, changes the intensity by concentrating or spreading the beam. Reducing spot size increases the intensity but reduces depth of focus, requiring better alignment and smooth gantry translation. Increasing spot size reduces intensity but reduces sensitivity to height variations and works for thicker materials. Practically, both should be optimized. First, a spot size should be chosen which is appropriate for the fabric and resolution, then set the power and traverse speed to achieve the required intensity and cut time with minimal to no damage to the fabric.

Cutting speed, meaning the speed at which the gantry head traverses over the fabric, has as much impact on cutting quality as spot size and intensity. When the cutting speed is too slow, this leads to excessive thermal input onto the fabric, which may cause burning, melting, or distortion of textile edge. The result of those effects is large kerf width, meaning wider cuts, and overall low accuracy cutting.

On the other hand, if the cutting speed is too fast, the beam does not deposit enough energy per unit length to fully sever the fabric. This may result in incomplete cuts and uncut fibers at the bottom of the cut. This means that either the laser power should be increased, the spot size should be decreased, or the cutting speed should be reduced. [31]

3.3.5 Optical Design Calculations

When combining our lens into a system we can utilize Zemax OpticStudio to get an idea of our beam behavior due to our lenses and subsequent coatings. This software does not allow us to account for the initial beam shape due to the use of a laser diode or account for the addition of the anamorphic prism pair. Our beam expansion system gives us a magnification of -7.8 shown below, resulting in a diverging beam 7.8 times its initial size. High magnification was desired due to the assumption that the initial beam size will be in micrometers.

$$Magnification = M = \frac{Back\ Focal\ Length\ (Bi - Convex)}{Back\ Focal\ Length\ (Plano - Concave)} = \frac{198.4}{-25.4} = -7.8$$

With Zemax software we can find the amount of power incident on the mirrors using the physical optics propagation function. The following calculations account for the loss of our singular lens that is not coated. Using the irradiance formula below and the information provided by our Zemax shown in Figure 24, we can find a max power of 5.45 milliwatts per pixel, with each pixel corresponding to 0.76 millimeters due to the graph having 5 pixels per 3.8 millimeters. Using this ratio, we get 9.43 milliwatts per mm^2.

$$I_0 = Peak\ Irradiance, w = Beam\ radius, P = Power$$

$$I_0 = \frac{2P}{\pi w^2} => 7.96 * 10^{-3} = \frac{2P}{\pi \left(\frac{1.32}{2}\right)^2} => P = .00545\ Watts$$

$$\frac{5.45}{(.76)^2} => 9.43 \frac{mW}{mm^2}$$

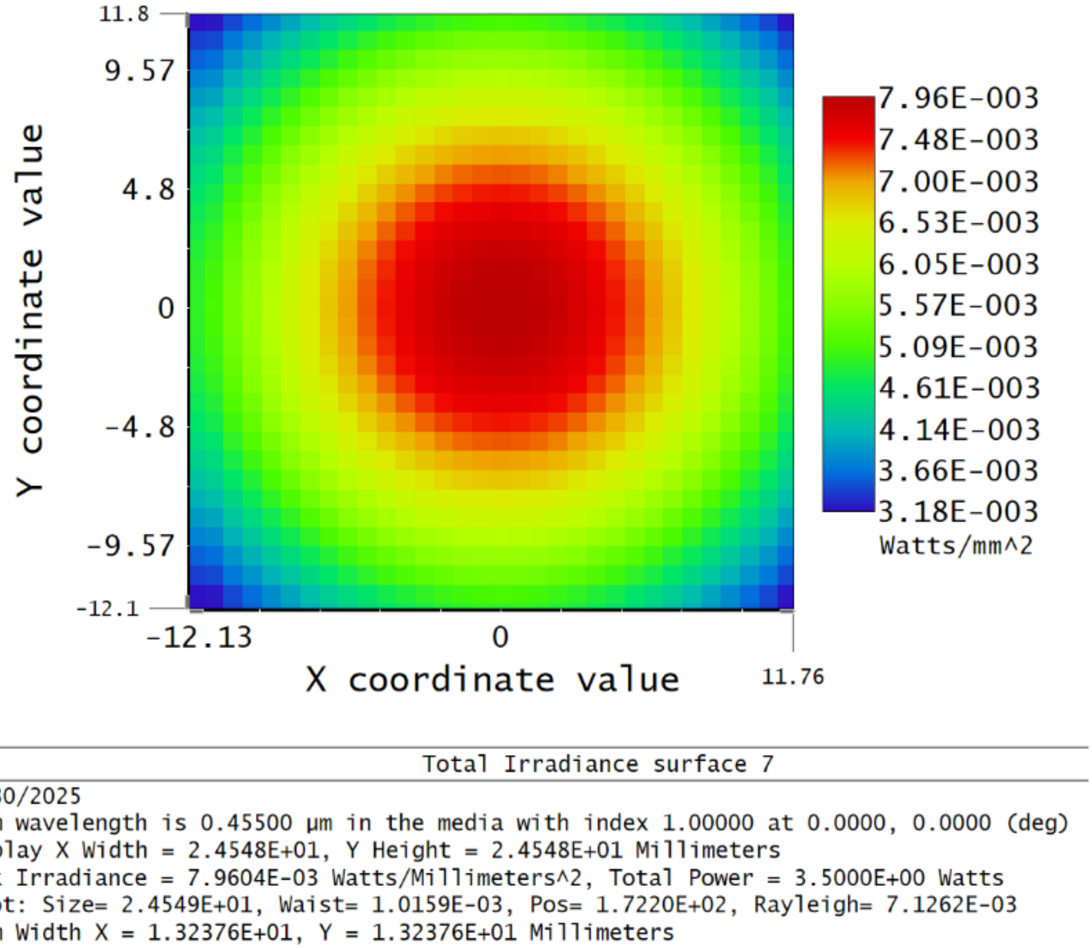

Figure 21: Beam Profile via Zemax

3.3.6 Image Acquisition and Processing

The imaging system is designed to operate with a camera mounted overhead, facing directly down toward the working field. During operation, the fabric will be laid flat within this field, ensuring that the entire working area is captured in a single image. The gantry system will be positioned completely outside the camera's field of view during image capture to ensure the entire fabric canvas is unobstructed to the camera.

Over the imaging area, ambient lighting will be carefully controlled and sufficiently bright to provide uniform illumination across the entire surface of the fabric. Proper lighting ensures that fabric details, textures, and marker sketches are clearly visible, minimizing shadows or glare that could interfere with image analysis down the line. The contrast between the fabric and the marker lines is especially critical for accurate sketch detection. For initial testing and algorithm development, only black and white markers will be used, as their contrast against most fabrics simplifies image segmentation. As the system's reliability improves, additional marker colors may be introduced, including UV fluorescent markers. Using UV illumination, these inks allow for cuts with invisible sketches, meaning the final product would not have any visible marker residue and resulting in an overall cleaner appearance.

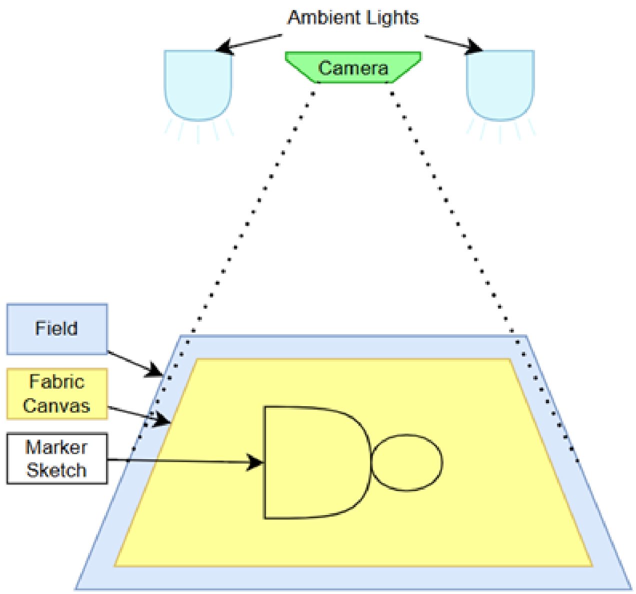

Figure 22: Schematic of the camera setup (not to scale and gantry out of frame)

Once the overhead image is captured, it will be transmitted to the Raspberry Pi for processing. The Raspberry Pi will execute a color-detection algorithm that identifies and stores the pixel coordinates of pixels which fall within the color threshold defined by the user. This information represents the approximate path of the user's sketch on the fabric.

Next, a path-generation algorithm will process the detected pixel data to compute a continuous path running along the center of the marker lines. This path extraction step effectively converts the sketch data into a vectorized format suitable for motion control. The resulting path coordinates can then be passed to the gantry system, which will trace and cut along these lines in a predefined sequence.

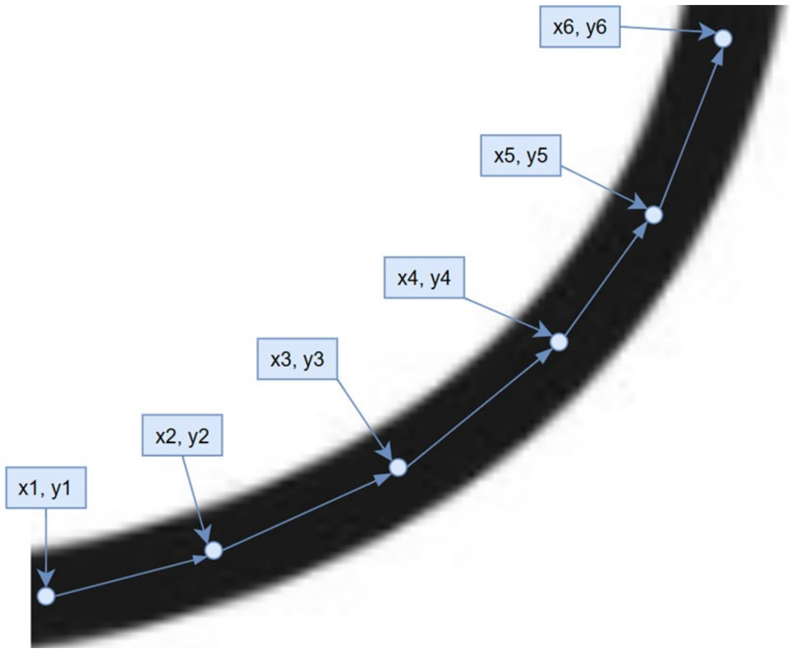

Figure 23: Simplified visualization of the ideal gantry path being generated along a simulated marker sketch.

3.3.6.1 Camera Selection

Since the project is using a Raspberry Pi Model 4B as the control board, the cameras that can be used are limited to the ones which are compatible with that type of board. Most of the other cameras listed on their website are not practical, such as the HQ Camera which requires extra lenses, though it would give the best quality images given proper lenses. The two main contenders are Camera Module 3 and Camera Module 3 Wide.

(https://www.raspberrypi.com/documentation/accessories/camera.html)

Table 16: Pi Camera Selection Comparison Table

Best Raspberry Pi Cameras		
Specifications	**Camera Module 3**	**Camera Module 3 Wide**
Sensor Resolution	4608 × 2592 pixels	4608 × 2592 pixels
Focus	Motorized	Motorized
Weight	4g	4g
Depth of Field	10 cm+, larger range of focus	5 cm+, shorter range of focus

Horizontal Field of View	66 degrees	102 degrees, image distorted at the edges
Vertical Field of View	48.8 degrees	67 degrees, image distorted at the edges
Price	$25	$35

Based off the table above, Camera Module 3 is the best option for the overhead camera. Also, given the height of the enclosure (600 mm), this is more than sufficient height for the camera to capture the entire field. In fact, if the field is 350 mm x 350 mm, the camera would have to be approximately 390 mm minimum above the field to capture the entire area.

$$\frac{350\ mm}{2\tan\left(\frac{48.8°}{2}\right)} = 385.79\ mm$$

This leaves sufficient room above the camera or below the field where components could be located.

After the camera captures the image, it will undergo image processing and path generation, which will direct the movement of the gantry system. As this system transfers from optics to software, image processing is expanded upon in Chapter 7.

3.3.7 Reflected Scattered Light Detection

3.4 Part Selection

Upon carefully researching and evaluating the project's needs and what is out there in the market, particular parts were identified to meet those needs. There was an emphasis on the project's design requirements and how well all of the parts would be able to integrate properly.

3.4.1 Motor Selection

Among the key features that were analyzed include movement precision, affordability, torque, current, and ease of use. Brushed and brushless motors were identified as not being able to meet the necessary position control necessary for the project. Servo motors and stepper motors were identified to provide desirable movement precision and control. Although servo motors do have some features that are superior to those of stepper motors, ultimately bipolar stepper motors with a hybrid rotor were chosen for the performance they provide with respect to their cost. It was also determined that certain components of the servo motor may not be necessary such as the use of an encoder.

A key feature of the stepper motor that stood out was the simple design of being able to count the short, incremental steps of the stepper motor to determine its position. Several stepper motors were analyzed to see which would best integrate into our project design. The project design will incorporate three stepper motors. One stepper motor for X-axis movement, one stepper motor for Y-axis movement, and finally one stepper motor for Z-axis movement. Being able to control three different axes is crucial to the effectiveness of the laser cutting through different materials.

When looking into the hybrid stepper motors available in the market, a variety of frame sizes are available. The most common that appeared in an internet search included NEMA 14, NEMA 17 and NEMA 23 stepper motors. The number "17" in NEMA 17 represents the faceplate dimensions of 1.7 inches by 1.7 inches or 57 mm by 57 mm. Of all the frame sizes available, the NEMA 17 was the most attractive as it offers a suitable size with respect to the desired size of the gantry system.

Table 17: NEMA 17 Stepper Motor Comparison

Stepper Motor Comparison			
Motor	17HE24-2104S	**17HS15-1504S1**	17HS08-1004S
Rated Current (A)	2.1	1.5	1.0
Step Angle (°)	1.8	1.8	1.8
Holding Torque (N*cm)	60.0	45.0	16.0
Dimensions (mm)	42x42x60	42x42x39	42x42x20
Weight (kg)	0.476	0.28	0.14
Cost (USD)	8.97	9.13	6.68

From the table above, several NEMA 17 stepper motors were compared. The key specifications that were closely analyzed included the rated current, the holding torque, and the dimensions. From these specifications, the last deciding factor was the cost effectiveness relative to what the motor offers. A key observation is that as the holding torque increases, the dimensions and weight also increase. The 17HS15-1504S1 bipolar stepper motor was chosen as it provided the ideal holding torque for the project design while also offering decent dimensions and weight.

3.4.2 Motor Driver Selection

Table 18: Motor Driver Comparison

Motor Driver Comparison			
Motor	A4988	**TB67S581FNG**	DRV8825
Operating Voltage (V)	8 - 35	8.2 - 44	8.2 - 45
Max. Continuous Current (A)	1.0	1.5	1.5
Peak Current (A)	2.0	2.2	2.2
Micro-stepping Resolution	Down to 1/16	Down to 1/32	Down to 1/32
Dimensions (mm)	15.24x20.32	15.24x20.32	15.24x20.32
Cost (USD)	8.95	6.95	15.95

3.4.3 Laser Diode Driver Selection

3.4.4 Optical Components Selection

Prior to the mirror system, we will be utilizing an aspheric lens, C140TMD-A, to bring all the laser diode light into the anamorphic prism pair, N-KZFS8, then using a beam expander made of a plano-concave lens and bi-convex lens, LC1975 and LB1945-AB, to expand the beam by a factor of at least 7 before reaching the mirrors.

Table 19: Mirror Selection (Highlighted)

Mirrors			
Specifications	**Fused Silica Broadband Dielectric (E02)**	**Protected Silver**	**Protected Aluminum**
Reflectivity (455 nm)	>99%	>97%	>90%
Bandwidth	Moderately broad 400nm - 750nm	Very broad 450 nm - 2 µm	Very broad 450 nm - 2 µm

Absorption	<1%	<3%	<10%
Laser Damage Threshold	High threshold (470 W/cm)	Moderate threshold (213 W/cm)	Low threshold, lot of power absorbed (43 W/cm)
Surface Quality	High quality, laser-grade, low scatter (10-5 Scratch-Dig)	Good quality, good for optics (40-20 Scratch-Dig)	Good quality, good for optics (40-20 Scratch-Dig)
Cost	Most expensive $50-$60	Least expensive ~$30	Moderately expensive ~$40

Table 20: Focus Lens Selection (Highlighted)

Aspheric Focusing Lens		
Specifications	**A280-A**	**354280-A**
Effective Focal Length (455 nm)	17.8 mm, slightly shorter	17.9 mm, farthest
Coating	AR (350 nm – 700 nm)	AR (350 nm – 700 nm)
Spot Diameter at Focal Point (455 nm)	11.256 µm aberrated spot size, not diffraction limited by airy disk, good quality	0.422 µm aberrated spot size, diffraction limited by airy disk with 3.608 µm diameter, best quality
Lens Diameter	6.5 mm	6.5 mm
Cost	$98.83	$83.90

Table 21: Camera Selection (Highlighted)

Best Raspberry Pi Cameras		
Specifications	**Camera Module 3**	**Camera Module 3 Wide**
Sensor Resolution	4608 × 2592 pixels	4608 × 2592 pixels

Focus	Motorized	Motorized
Weight	4g	4g
Depth of Field	10 cm+, larger range of focus	5 cm+, shorter range of focus
Horizontal Field of View	66 degrees	102 degrees, image distorted at the edges
Vertical Field of View	48.8 degrees	67 degrees, image distorted at the edges
Price	$25	$35

Chapter 4: Real World Design Constraints and Related Standards

4.1 Standards

4.1.1 Laser Safety Standards

When it comes to operating a laser many safety precautions should be taken to ensure safe operation. Laser classes and standards help us identify how we should be using and behaving around our lasers to ensure no one is harmed while making this fabric laser cutter system. We included considerations of the American National Standards Institute as well as Florida Administrative codes. For the laser safety classes, the potential hazard of the laser increases as the number increases. These hazards are considered in terms of harmful impacts towards our skin and eyes. Products including lasers must have a label listing the classification of the laser.

Lasers labeled Class 1 do not pose a threat of biological damage. This means it is not an eye, skin, or burn hazard. Class 1M contains lasers that do not produce hazardous conditions during normal operations, unless the laser is being viewed by an optical instrument. Class 2 lasers are within the visible spectrum of 400-700 nm and do not exceed 1mW in power. This class includes both continuous wave and pulsed lasers. The maximum duration for eye exposure during use of these lasers is .25 seconds, equal to human aversion responses, meaning you should not attempt to look at them. These lasers should not be viewed directly with optical instruments. 2M lasers are still in the visible spectrum and the human aversion response normally protects the eye for unaided viewing. These lasers are potentially hazardous if viewed with certain optic instruments [18].

Class 3 is split into 3B and 3R lasers that include lasers within the visible spectrum. 3R corresponds to lasers with a beam between 1 milliwatt and 4.99 milliwatts of power, so direct eye exposure should be avoided. Whereas class 3B lasers have a beam power of 5 milliwatts to 500 milliwatts, or half a watt, and any exposure to this beam should be avoided. This includes lasers that can harm your skin and materials if held long enough at close range. When considering exposure to beams from any class of laser, include considerations of stray or reflected beams.

Class 4 lasers are the biggest concern, as these need-controlled measures to prevent exposure from the direct beam or a reflected beam. These lasers have the potential to ignite and create fire, causing airborne byproducts or materials. These lasers are greater than a half of watt of power and pose a threat to your skin and materials from burns. Do not stare at these lasers even when the laser dot is on another surface, and the light can be bright enough to cause a sustained afterimage lasting longer than 10 seconds. If this sustained afterimage occurs, laser light is too bright [19]. When operating any laser, it can be useful to have a laser safety officer contact to ask questions regarding your specific setup or design.

4.1.2 Software Development Standards

Software reliability is important since incorrect logic or latency can directly impact laser safety. The C/C++ firmware running on the Raspberry Pi Pico 2 follows guidelines derived from MISRA-C:2012, which restricts unsafe operations such as dynamic memory allocation (rule 21.3) and enforces strict type-safety rules (rules 10.1 - 10.8, 11.3-11.5). This minimizes the risk of undefined behavior in real-time execution which will help with lowering latency.

4.1.3 Communication and Interface Standards

As established in chapter 3, the evaluation of communication interfaces determined UART to be the most suitable protocol for linking the Raspberry Pi 4B supervisory computer with the Raspberry Pi Pico 2 real-time controller. Communication between these devices is implemented through a UART serial interface compliant with the **EIA/TIA-232** signaling specification. UART was selected for this link due to its simplicity, determinism, and low resource overhead, which make it ideal for real-time embedded communication. The protocol requires only two signal lines (TX and RX), transmits data asynchronously without a shared clock between the sender and receiver, and provides predictable timing behavior which is an essential feature for the precise coordination of laser and motion control subsystems.

Compared to more complex alternatives such as USB or I²C, **UART avoids driver negotiations and bus arbitration, reducing latency and software complexity**. Its compliance with the EIA/TIA-232 standard ensures robust, industry-recognized data framing (start and stop bits, optional parity) and voltage-level compatibility while also allowing straightforward monitoring through standard serial-monitor tools. This ease of visibility greatly aids debugging, diagnostics and long-term maintenance.

Additionally, the USB 2.0 interface on the Pico 2 adheres to USB-IF specifications, supporting save device enumeration, firmware flashing, and regulated power delivery. These standardized interfaces collectively enhance interoperability, simplify system integration, and preserve data integrity between the Linux-based supervisor (Pi 4B) and the bare-metal controller (Pico 2). The resulting communication architecture is both reliable and modular, enabling future subsystems without requiring major firmware redesign.

Chapter 5: Application of LLMs

5.1 ChatGPT

5.1.1 Assistance

ChatGPT has emerged as a transformative modern tool, reshaping research and development workflows in a manner reminiscent of the handheld calculator's impact on engineering education decades ago. With the introduction of Model 5, its capacity for technical reasoning, data organization, and natural-language coding assistance has made it especially valuable for multidisciplinary engineering projects such as ours. Throughout this project, ChatGPT was used not merely as a conversational assistant but as a codesign partner supporting decision-making, code generation, literature review, and design choices such as name selection and logo design.

5.1.2 Part Selection Assistance

In the early phases, ChatGPT assisted in comparing potential system architectures for the Fabric Laser Cutter System (F.L.C.S), evaluating platforms such as the Raspberry Pi 4B, Pi 5, Jetson Nano, ESP32, and Arduino Mega 2560. The comparison data it provided included numerous technical specifications such as processor speeds, connectivity, and power requirements which offered a solid baseline for evaluation. However, it quickly became clear that these numbers could not be accepted at face value. As accurate as Model 5 often is, it remains susceptible to occasional errors.

To ensure reliability, we conducted independent verifications of the specifications that ChatGPT provided, consulting official datasheets, manufacturer documentation, and vendor product listings. Most of the values aligned closely with ChatGPT's output, confirming its usefulness as a research accelerator. Yet, certain parameters such as latency performance, real-time responsiveness, and power draw under load were difficult to confirm since they were either not specified in the datasheets or varied by testing environment. These cases required additional investigation.

This process underscored a critical lesson about using AI tools in engineering research: while ChatGPT can rapidly synthesize complex technical data, human validation remains essential. The model's role is best seen as a guide, not an absolute authority. By crosschecking every specification and reconciling inconsistencies, the team ensured that each design decision was grounded in verifiable data rather than unverified model output.

5.1.3 Assistance in Code Generation and Web Development

During the implementation phase, ChatGPT played an important role in the development of the project's website, which serves as a digital interface for documentation and demonstration. Initially, I began constructing the website using basic HTML and CSS, relying on the guide provided in order to understand page structure and styling. However, these early attempts lacked organization and consistency, often requiring time to adjust the layout of the website.

ChatGPT streamlined this process by providing step-by-step guidance and example code structures that aligned with modern web-development standards. It explained how to properly format HTML documents, apply CSS for layout control, and organize content sections for clarity.

The biggest help yet was how to integrate our project documents into the website. As of right now the website is in its infancy with not much to look at. However, it provides an easy-to-access hub for all our documents as we work toward our final submission and presentation. By creating a single, centralized platform, ChatGPT made it easier to host progress updates, link technical files, and maintain version control throughout the development process.

As the project continues to grow, the foundation built through ChatGPT's guidance will allow for smoother expansion into interactive elements, and visual media integration. This early groundwork not only improved efficiency but also ensured that the website remains structured, scalable, and reflective of the team's professional standards.

5.1.4 Assistance in Literature Review and Research

Beyond technical implementation, ChatGPT also served as an effective tool for conducting and organizing literature obtained from google scholar or its own recommendation. During the research phase, it was used to identify credible sources, summarize technical papers, and clarify complex topics relevant to our system's design such as display latency, and real-time processing on embedded Linux. By providing a link from google scholar and prompting the model with targeted questions, it was possible to generate clear explanations and summaries of engineering concepts that would otherwise require extensive manual searching.

Additionally, ChatGPT aided in the citation and documentation process by suggesting how to reference online articles, technical datasheets, and manufacturer documentation.

Whether the task involved citing a paper within a paragraph or determining what information could be appropriately referenced, ChatGPT provided accurate guidance that helped maintain consistency while avoiding legal trouble that could be present when reference another's work.

In summary, ChatGPT's contribution to the literature analysis lay in its ability to synthesize information, improve organization, and accelerate understanding. It functioned as a research assistant capable of guiding exploration without substituting critical analysis. This integration of AI into the research workflow not only enhanced productivity but also strengthened the depth and quality of the project's foundation.

5.1.5 Assistance in Design Choices

ChatGPT also played a role in the creative design process, particularly selecting the project's name and developing a logo. Early in the project, several names were proposed, but many lacked technical relevance or did not reflect the system's function. Eventually we landed on Cutting Laser for Optimized Textile Handling (C.L.O.T.H); but that too did not truly reflect our project as it lacked the clarity needed for an outside reviewer to get a sense of what the project is about. As a replacement, ChatGPT generated ideas such as the friendly name "Draw2Cut" and the attractive name "VisionCut"; eventually the final acronym F.L.C.S (Fabric Laser Cutter System) was chosen to represent us as it best captured the project's focus and professional tone.

In addition to name exploration, ChatGPT contributed to the logo design process by generating potential designs that could represent our system. This was one of the most impressive aspects of ChatGPT as the generated designs were clean, simple, and functional. With additional prompts regarding color, depth, and style, ChatGPT was able to present the final logo concept that now represents the entire project.

Overall, ChatGPT's involvement in these design choices simplified the brainstorming phase and provided quick, clear feedback on visual and conceptual direction. While the final designs were adjusted by hand, the model's input helped narrow down options and maintain our identity.

5.1.6 Conclusion

Throughout the development of the Fabric Laser Cutter System (F.L.C.S.), ChatGPT proved to be a versatile, reliable, and valuable tool that supported the team in multiple aspects of the project. From assisting in part selection and website development to organizing papers and refining the project's identity, it enhanced both technical efficiency and creative direction.

Despite its strengths, ChatGPT was not without limitations. Some of the information it produced required verification, and certain outputs needed refinement to align with the project's real world constraints. Nevertheless, its integration into the workflow demonstrated how AI can act as a capable partner that amplifies human effort rather than replacing it.

Overall, ChatGPT's inclusion in this project not only improved productivity and organization but also offered a peek at the future use of large language models with engineering design, research, and documentation.

Chapter 6: Hardware Design

6.1 Optical Design

6.1.1 Optical Design Prior to Mirrors

Below is an optical schematic of the lens system without the anamorphic prism pair demonstrating the expansion of the beam after the bi-convex lens. Although the beam initially expands, it become nearly collimated after around 200 millimeters or 7.8 inches. This was intentional as it allows us the needed space to build the mirror system such that it does not impact our laser lens system and has enough room to move and change position before the beam reaches the focusing lens. To compensate for the anamorphic prism pair, a blank space of around 30mm was placed between the aspheric and plano-concave lens.

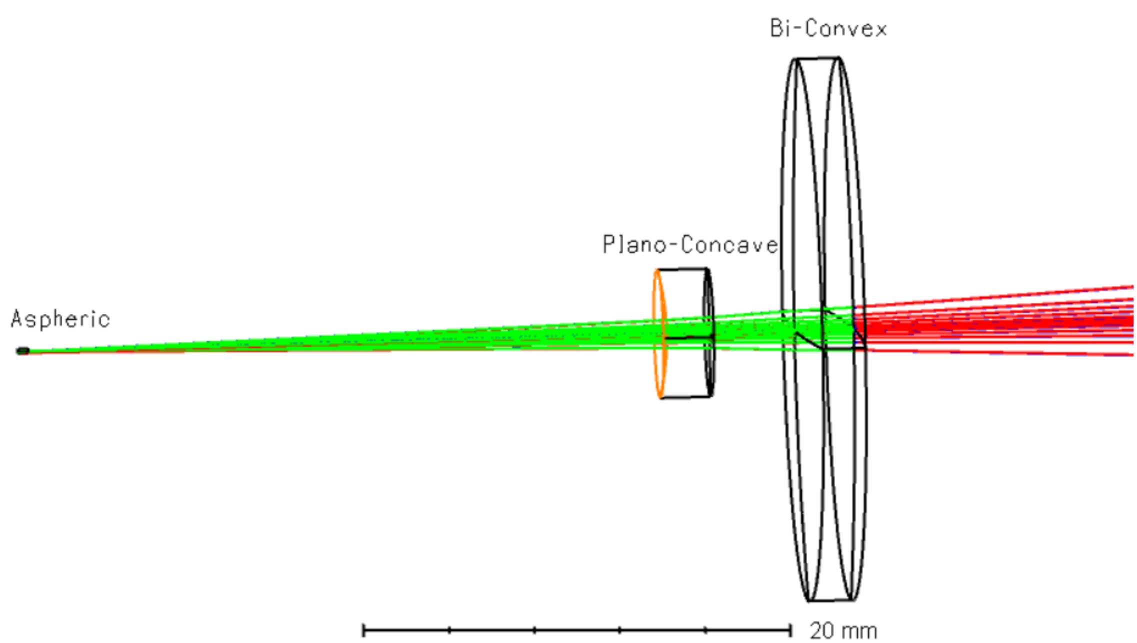

Figure 24: Lens Diagram via Zemax

6.1.1 Optical Design: Mirrors and Focusing Lens

The mirrors and the focusing lens are the main system contributing to the redirection of the beam onto the desired spot to be cut. The design will use two dielectric E02 coated mirrors to direct the beam in the x and y positions of the fabric canvas, given that the beam is entering the gantry and hits the first mirror horizontally. Below the second mirror is the aspheric focusing lens, 354280-A, which can be adjusted vertically to adjust where the focal spot is vertically. This can be adjusted based on the thickness and type of fabric, which can vary.

Chapter 7: Software Design

7.1 Optimal Programming Languages

Several programming languages can be used for image processing and gantry path generation. The most common languages for this purpose are Python, C++, C, Rust, and MATLAB. Python, through libraries such as OpenCV, NumPy, and many others, offers a high-level, intuitive approach to processing images and extracting relevant features. C++ also supports OpenCV and could execute the same image processing programs significantly faster due to its compiled nature and lower-level memory management. Rust, though newer, provides strong performance and safety precautions which could prevent common programming errors such as memory leaks. C is extremely efficient for embedded systems, but due to the lack of native high-level libraries, image processing becomes cumbersome and so would not be an ideal language. MATLAB, while great for prototyping and algorithm testing, due to its heavy runtime and licensing constraints, would not be suitable for use in a real-time embedded environment such as a Raspberry Pi.

Table 19: Programming Language Comparison Table

Programing Language				
Specifications	**Python**	**C++**	**C**	**Rust**
Recommended Compiler	CPython	GCC	GCC	rustc
Runtime Performance	Very slow, high overhead	Fast	Fast, low overhead	Fast and optimized
Complexity	Easy and intuitive	Like C, but less complex/basic	Complex and low level	Strict syntax, ownership model

Computer Vision and Image Processing	Extensive number of dedicated libraries (OpenCV, NumPy, SciPy, TensorFlow, many more)	Variety of libraries (OpenCV, Dlib, VXL, VIGRA)	Very limited, would require custom code	Limited, could use Open CV
Memory efficiency	Poor, high overhead	Good	Excellent, direct access to memory	Safe and efficient
Error handling	Safe	Needs manual management	Prone to errors	No nulls, enforced checks
Hardware control	Possible through libraries	Can access hardware efficiently	Excellent, direct hardware access	Safe low-level access

For image processing and generating gantry paths, the optimal programming language would be Python, at least during early development. Python integrates seamlessly with the Raspberry Pi OS, has native support for the camera through libraries such as picamera2 and OpenCV. Its simplicity makes it ideal for tuning thresholds, filtering noise, and identifying marker coordinates before converting them into a usable path. However, Python's major drawback is runtime performance due to being a very high-level language. This can cause severe lag when handling large images or complex operations. For real-time operation, the image processing program could later be converted to C++.

7.2 Possible Bugs and Solutions

Running into bugs during image acquisition, path generation, and all the steps in between are inevitable. Being able to identify and mitigate these errors in the best way possible is the best defense against the system unexpectedly malfunctioning or breaking. With all the risks of managing a high-power laser, an extremely high intensity spot of light, potentially flammable fabric, and operating delicate components, it is optimal that these bugs can be caught and dealt with and completely avoided ahead of time before they cause any real damage.

Chapter 8: Optoelectronics Feasibility Study

8.1 Laser Diode

Our laser diode requires an operating voltage of 4.4-5.2 volts and a typical operating current of 2.1 amps. Our laser diode driver will ensure that the maximum operating current of 3 amps is not reached, as that would burn out our laser diode. We will be using an aluminum heat sink to ensure the laser diode does not exceed temperature threshold limits.

8.2 Image Acquisition System and Focusing Lens

Chapter 9: Integration and Testing Plan

9.1 Integration

The main goal of this project is to successfully integrate our subsystems so they may operate smoothly to carry out their functions. We will be utilizing a photodiode system to measure reflectance returning to the lens system while it is cutting the fabric. The image acquisition system will collect data regarding the location of the fabric to be cut, and this information will be communicated to the mirror system to direct the beam. The power system will supply power to our components, including the laser system which will be dormant until the touchscreen communicates to start a cut.

9.2 Testing

When preparing for our demo we plan to meet each week in the month of November, in person, to prepare and gather our components. This will include testing our laser diode with our lens system as well as our touchscreen, gantry system, and focusing lens.

Chapter 10: Administrative Content

10.1 Work Distribution

Table 17: Work Distribution Table

Computer Engineering	
Nolphky Nicolas	***Responsible for:*** Touchscreen subsystem Controller and sub-controller Implement serial communication HMI Interface
Electrical Engineering	

Anthony Martinez-Garcia	***Responsible for:*** PCB design Motor research and selection Motor driver research and selection Laser diode driver research and selection Design power supply unit
Photonic Science and Engineering	
Jacqueline Harper	***Responsible for:*** Facilitating group meetings and encouraging time management Group document formatting Project motivation and background Laser diode system with beam expansion lenses and prism pair Integration of LD system into housing Housing selection Laser Diode System Feasibility Study
Mike Rodriguez	***Responsible for:*** Mirrors for guiding beam Final focus lens onto the fabric Image acquisition and gantry path generation Photodiodes for scattered beam light detection

10.2 Budget and Financing

This project is not sponsored and is funded by the students who complete each subsystem. The budget sets a target to keep costs below a certain price while not compromising on quality. Total cost is kept in mind to make the final product affordable to a common customer. The budget could change due to design changes or economic factors such as a tax on imported goods.

10.3 Bill of Materials

The table below shows the components that make up the bill of materials.

Table 21: Bill of Materials

Item	Details	QTY	Price (USD)
Raspberry Pi 4/4GB	Main processor for touchscreen HMI	1	55.00

Raspberry Pi Touch Display 2	Main touchscreen	1	81.95
Pi Bezel for 7" Pi touchscreen	Frame for the touchscreen (optional, 3d printing)	1	9.99
Samsung PRO Endurance (256GB)	Internal storage for the touchscreen	1	29.99
Passive Buzzer	Provides feedback for user actions and errors	1	0.95
standoffs and screws	Standoffs, screws, etc	1	14.95
Touchscreen Power (TBD)	Powers the touchscreen (integrated into system PSU)	TBD	TBD
Laser Diode	Burns/Cuts fabric	1	75.00
Aspheric Lens	Collimates beam into prism pair	1	104.30
Anamorphic Prism Pair	Shapes the beam	1	202.10
Plano-Concave Lens (Lens 1 of Beam Expander)	Expands beam	1	28.00
Bi-Convex Lens (Lens 2 of Beam Expander)	Nearly collimates beam	1	45.00
Focusing Lens	Focuses laser beam	1	TBD
Lens Holders and Mounts	3D Printed	4	Filament Costs
Housing/Enclosure	Holds components together in with easy to use features	1	180.00 + Shipping

10.4 Project Milestones

Below are two tables that outline timeframes for tasks to be completed in Senior Design 1 and Senior Design 2. The project is broken into several parts that will come together to realize a final product. Breaking the project into smaller parts allows for weekly progress to be made by a certain timeframe.

Table 182: SD 1 Project Milestones

Senior Design 1 (Fall 2025)					
Week (s)	**Milestone:**	**Assigned to:**	**Start Date:**	**End Date:**	**Progress:**
1	Form Project Idea	Everyone	8-19-25	8-25-25	DONE

2	Form Group	Everyone	8-26-25	8-28-25	DONE
2/3	Reach Out to Reviewers	J. Harper, A. Martinez-Garcia, N. Nicolas	8-29-25	9-4-25	DONE
3	Complete Divide & Conquer Initial Draft (Submit)	Everyone (M. Rodriguez)	9-2-25	9-5-25 (noon)	DONE
4	Senior Design Bootcamp	Everyone	9-9-25	9-12-25	DONE
4	Create Project Website	N. Nicolas	9-8-25	9-28-25	DONE
4	Equipment Loan (if needed)	Everyone	9-8-25	9-12-25	DONE
5	Divide & Conquer Final Revision (Submission)	Everyone (A. Martinez-Garcia)	9-8-25	9-12-25 (noon)	DONE
7	Email D&C to Reviewers (add to Website)	A. Martinez-Garcia, (N. Nicolas)	9-12-25	9-19-25	DONE
7	5 Pages Completed (total, per person, Deadline by J. Harper)	Everyone	9-30-25	10-2-25	DONE
8	Optical Demo	J. Harper, M. Rodriguez	9-27-25	10-7-25 (10AM SHARP)	DONE
8	10 Pages Completed (total, per person, Deadline by J. Harper)	Everyone	9-29-25	10-9-25	DONE
9	15 Pages Completed (total, per person, Deadline by J. Harper)	Everyone	9-29-25	10-16-25	DONE
10	20 Pages Completed (total, per person, Deadline by J. Harper)	Everyone	9-2-25	10-25-25	In Progress
11	(Submit) Midterm Report First Draft	Everyone (J. Harper)	9-2-25	10-31-25 (noon)	DONE
12	Midterm Report Meeting	Everyone	11-3-25	11-5-25	DONE
12	(Submit) Midterm Report Revision	Everyone (N. Nicolas)	11-3-25	11-7-25 (noon)	DONE
13	25 Pages Completed (total, per person, Deadline by J. Harper)	Everyone	9-29-25	11-14-25	In Progress

13	Final Optical Demo	J. Harper, M. Rodriguez (Everyone Present)	11-18-25	11-18-25 (10AM SHARP)	TBD
14	30 Pages Completed (total, per person, Deadline by J. Harper)	Everyone	9-29-25	11-21-25	In Progress
14	Upload report and video (YT Link) to website + email for Reviewer Feedback	(N. Nicolas) A. Martinez-Garcia	11-17-25	11-21-25	TBD
15	(Submit) 120-page Final Report	Everyone (A. Martinez-Garcia)	9-2-25	11-25-25 (noon)	In Progress
15	(Upload) Demo Video	Everyone (A. Martinez-Garcia)	11-17-25	11-25-25 (noon)	TBD
15	Upload Demo to Website and Email to Committee	N. Nicolas	11-17-25	11-25-25	TBD
15	Submit Evaluations	N. Nicolas	11-17-25	11-25-25	TBD

Table 193: SD 2 Project Milestones

Senior Design 2 (Spring 2026)					
Week (s)	**Milestone:**	**Assigned to:**	**Start Date:**	**End Date:**	**Progress:**
1	Purchase Components	Everyone	9/25	2/26	In Progress
TBD	Test Experimental Setup, Adjust	Everyone	TBD	2/26	TBD
TBD	Assemble Housing	Everyone	TBD	3/26	TBD
TBD	CDR Video Submission	Everyone	1/26	1/26	TBD
TBD	CDR Video on Website and Sent to Committee	N. Nicolas	1/26	2/26	TBD
TBD	Review Final Submission Documents with Committee	Everyone	TBD	3/26	TBD
TBD	Upload all Documents to Project Website	N. Nicolas	3/26	Final Exam Date	TBD

Appendices

Appendix A – References

[1] “Buildlog.net 2.x Laser”. *Buildlog.Net Blog*, https://www.buildlog.net/blog/2011/02/buildlog-net-2-x-laser/. Accessed 1 Sep. 2025.

[2] “Epilog Fusion Pro Lasers”. *Innovative Cutting Systems*, https://www.innovativecuttingsystems.com/epilog-laser/fusion-pro-laser-series.ht m. Accessed 1 Sep. 2025.

[3] “GFL FIBER LASER”. *Dener Machinery*, https://dener.com/catalog/Gantry_Fiber_Laser.pdf. Accessed 10 Sep. 2025.

[4] “Wattsan 6090 LT”. *Wattsan*, https://wattsan.com/product/wattsan-6090-lt/?srsltid=AfmBOory9nmu9Siww-hZrptmbuj_zTc-xi6FvI4JbPgQV08FTDa5Ga4x. Accessed 10 Sep. 2025.

[5] Felipe Mosquera, A. M., Kavinaash Jesurajah, Jackson Gilliland, Nolan McGinley, Amir Mohd (2024). "UCF Senior Design Group 5 Fall 2023 - Spring 2024." from https://www.ece.ucf.edu/seniordesign/fa2023sp2024/g05/.

[6] J.L. Perry, J. H. A., R. Vijayakumar (2016). Submicron and Nanoparticulate Matter Removal by HEPA-Rated Media Filters and Packed Beds of Granular Materials**:** 28.

[7] 7*inch HDMI LCD (C) - Waveshare Wiki.* (n.d.). https://waveshare.com/wiki/7inch_HDMI_LCD_(C)

[8] Elecrow. (n.d.). *RC070M 7 inch 1024 x 600 Touch Screen Display with 720P Camera for Raspberry Pi/MacBook Pro./ Windows 10 – Elecrow Wiki.* https://www/elecrow.com/pub/wiki/rc070m-7-inch-1024-x-600-touch-screen-display-with-720p-camera-for-raspberry-pi-macbook-pro-windows-10.html?h=7

[9] Raspberry Pi Ltd. (2025). *Raspberry Pi Touch Display 2 Product Brief.*

https://datasheets. Raspberrypi.com/display/touch-display-2-product-brief.pdf

[10] *Touch Display 2.* (n.d.). https://www.raspberrypi.com/documentation/accessories/touch-display-2.html

[11] Pounder, L. (2024, November 4). *Raspberry Pi Touch Display 2 Review: A Touch of class.* Tom’s Hardware. https://www.tomshardware.com/raspberry-pi-touch-display-2-review-a-touch-of-class

[12] Dean McClements, A. L. (2022, 2024). "CO2 Laser Vs. Fiber Laser: The Main Differences." from https://www.xometry.com/resources/sheet/co2-laser-vs-fiber-laser/?utm_source=chatgpt.com.

[13] Verdeyen, J. T. (1995). Laser Electronics, Prentice Hall: 74.

[14] El Sherif, M., et al. (1997). "Prediction of absorbance from reflectance for an absorbing-scattering fabric." Color Research & Application **22**(1): 32–39.

[15] Liu, Y., et al. (2010). "UV/visible/near-infrared reflectance models for the rapid and non-destructive prediction and classification of cotton color and physical indices." Transactions of the ASABE **53**(4): 1341–1348.

[16] Lasers, R. (2024). "Why a Larger Beam Results in a Smaller Spot Size in Laser Designation?". from https://www.rpmclasers.com/blog/why-a-larger-beam-results-in-a-smaller-spot-size-in-laser-designation/.

[17] Ng, B. (2023). "Laser Beam Expanders: Keplerian vs. Galilean Beam Expanders and Other Configurations." from https://wavelength-oe.com/laser-beam-expanders-keplerian-vs-galilean/.

[18] Safety, U. E. H. a. "Laser Safety Manual." from https://www.unf.edu/ehs/policies/laser-safety-manual.html#:~:text=UNF:%20Laser%20Safety%20Manual

[19] Hadler, J. (2023). "Laser Safety Facts." from https://www.lasersafetyfacts.com/laserclasses.html#:~:text=Laser%20classes,for%20updated%20info%20April%202023.

[20] Cerqueira, F., Brandenburg, B., & Max Planck Institute for Software Systems (MPI-SWS). (n.d.). A comparison of scheduling latency in Linux, PREEMPT RT, and LITMUS RT. *Abstract*. https://people.mpi-sws.org/~bbb/papers/pdf/ospert13.pdf

[21] https://www.thorlabs.com/newgrouppage9.cfm?objectgroup_id=139&pn=BB03-E02

[22] https://www.thorlabs.com/newgrouppage9.cfm?objectgroup_id=3810

[23] https://www.opmtlaser.com/laser-galvanometers/)

[24] https://www.popularwoodworking.com/techniques/what-why-hows-of-cnc-machines/

[25] https://www.thorlabs.com/newgrouppage9.cfm?objectgroup_id=6430

[26] https://www.edmundoptics.com/f/sill-optics-f-theta-lenses/40163/

[27] https://www.edmundoptics.com/knowledge-center/application-notes/lasers/gaussian-beam-propagation/?srsltid=AfmBOoq8YUaQ3TCxzE1MoZ7RZCdAx4hO-KCN_3dgRsXpdhulatVNL20k

[28] https://www.ipgphotonics.com/newsroom/stories/why-should-we-care-about-spot-size-in-fiber-laser

[29] https://www.thefabricator.com/thefabricator/article/lasercutting/the-importance-of-focal-positions-in-laser-cutting

[30]https://www.xometry.com/resources/sheet/laser-parameters/, https://www.thunderlaser.com/choose-by-industries/the-impact-of-laser-on-the-fabric1/

[31]https://www.researchgate.net/publication/258105599_A_study_on_laser_cutting_of_textiles